Università di Pisa

DIPARTIMENTO DI BIOLOGIA

Corso di Laurea Magistrale in Biologia applicata alla Biomedicina

Tesi di laurea magistrale

Modelling of the functional amyloid aggregation at the synapse

New insights into the local computational properties of neurons

Candidato:
Michele Sanguanini
Matricola 481810

Relatore:
Prof. Antonino Cattaneo

Correlatori:
Prof. Vittoria Raffa
Prof. Massimo Dal Monte

Anno Accademico 2014–2015

Contents

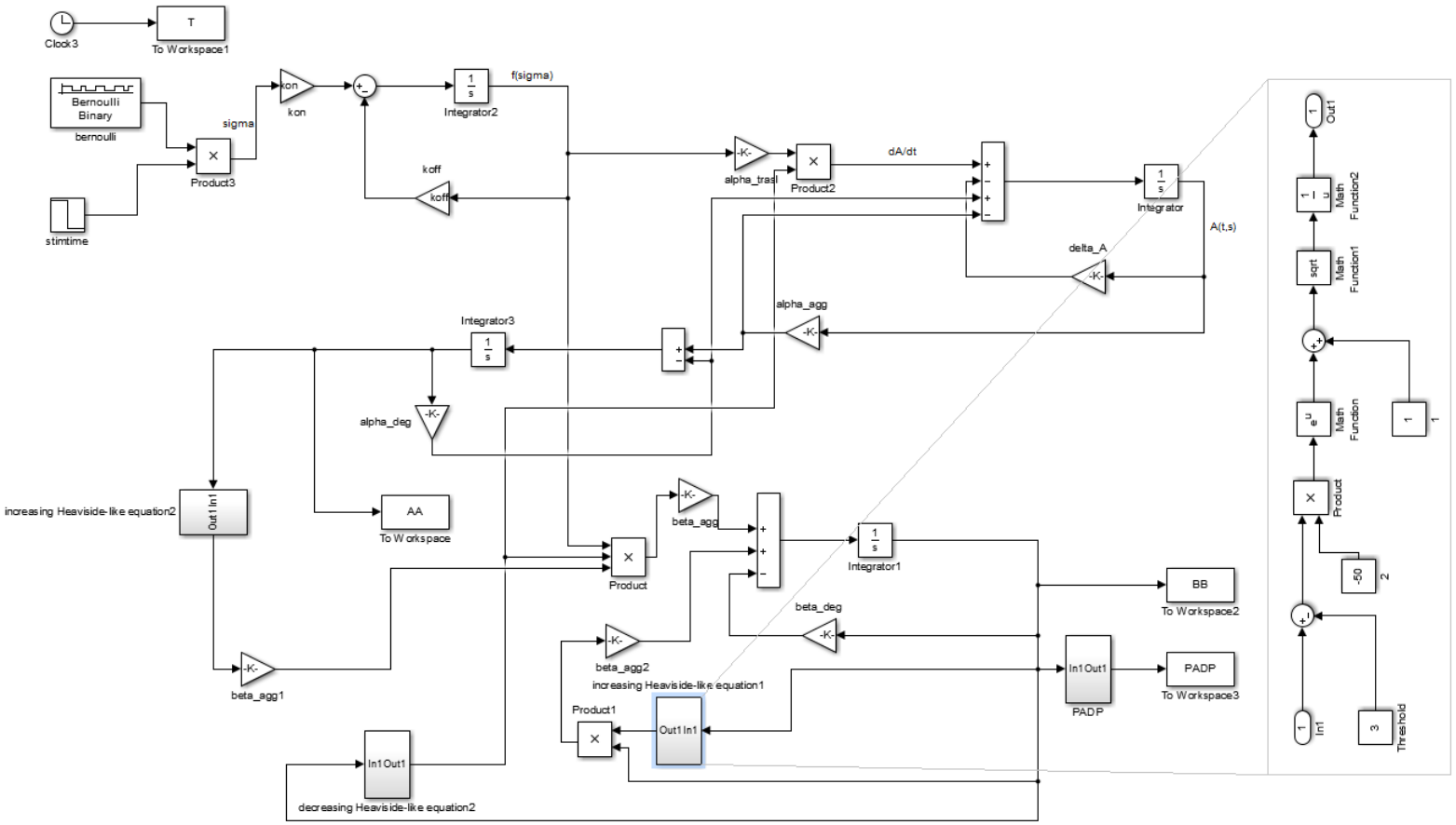
Clock3
T
To Workspace1
Bernoulli Binary
bernoulli
stimtime
Product3
sigma
kon
kon
Integrator2
f(sigma)
koff
koff
alpha_trasl
Product2
dA/dt
Integrator
A(t,s)
delta_A
alpha_agg
Integrator3
alpha_deg
increasing Heaviside-like equation2
AA
To Workspace
beta_agg
Product
Integrator1
BB
To Workspace2
beta_deg
beta_agg1
beta_agg2
increasing Heaviside-like equation1
Product1
PADP
To Workspace3
decreasing Heaviside-like equation2
Out1
Math Function2
sqrt
Math Function1
Math Function
Product
-50
2
1
Threshold
3
In1

Acknowledgments

First, I would like to thank my supervisor Prof. Antonino Cattaneo for helping me to give order to my ideas on the still obscure and fascinating molecular world of functional amyloids. I would also like to thank my co-tutors Prof. Vittoria Raffa, in particular for her useful observations on the parameter stability of the model, and Prof. Massimo Dal Monte.

I would like to thank Prof. Armando Bazzani, Prof. Annalisa Pastore, Prof. Brunello Tirozzi and Fabrizio Londei for useful discussions.

I am grateful to all the people that are accompanying me through all these years of intense personal and academic formation: the Biologists' group of Collegio Faedo (Vigji, Mark, Lale, Jackie, Christie, Cate, Capo, Ale), the people at the Bio@SNS lab (just to mention a few, Cristina Di Primio, Valentina Quercioli, Giacomo Siano, Marco Terrigno, Antonella Calvello, Roberto Ripa, and prof. Alessandro Cellerino), and last–but not least–the group of Dr Gian Michele Ratto at the NEST laboratory. A special thought goes to the friends of the Lübecker Guesthouse–Wendelien, Dominik, Jelena, Li-Fan, Ilaria, Shana and Tianyu–and to all the people at the Institut für Integrative und Experimentelle Genomik at the University of Lübeck, in particular Jaafar Al-Hasani and Maria Segura Puimedon. I thank also Raffaella Tallarico, Margherita Fantoli, Matteo Vezza, and Alessandro Monti for the nice time we spent together.

Ringrazio i miei genitori per il supporto che mi hanno sempre donato e che mi sta permettendo di costruire con serenità la mia strada–ma li ringrazio soprattutto per la (molta) pazienza con la quale mi hanno sopportato per tutti questi anni!

Dulcis in fundo, I would like to thank Saverio, he knows the reason why.

Chapter 1

Introduction

1.1 The molecular basis of memory and learning

Memory and learning are two strictly related concepts, the former being generally defined as the ability of a system to retain, store and recall the input information, the latter as the ability of a system to modify its behavior according to the previous experience [1]–that is the time series of the inputs to the system.

Starting from the early reports from amnesic patients (as reviewed in [2]), many distinct systems of memory have been recognized–e.g. episodic memory of facts and events, habits and other forms of non-declarative memory. A review of the different systems of memory is above the aim of this introduction, however some fundamental aspects should be kept in mind before approaching the problem of molecular basis of memory [2]. The first assumption, which is fundamental for molecular neurobiology in general, arguably constitutes the fundamental principle of molecular memory and is the following:

> Neural circuits are the substrate for the processing, storage, and retrieval of information in the nervous system [3, 4].

From this principle it reasonably derives that different forms of memory require different computation properties of the neural system. For example, while declarative memory is meant to be a record of personal experience (which is unique in space and time), non-declarative memory aim is to detect recurrences from a series of distinct events. The different functional requirements of each memory system likely underlie different molecular characteristics, although sharing a common molecular baseline–such as the PKC

calcium-dependent kinases, or the mTORC signaling.

In any case, the complexity of the interactions between learning, memory retrieval and memory assessment requires some methodological caution while trying to classify systematically memory systems and their molecular phenomena [2]. There are in fact growing evidences, from both animal models (i.e. from an evolutionary point of view) and human patients, that tend to fade the boundaries between the canonical divisions of declarative and non-declarative memory, and between the the partitioning of non-declarative memory systems.

1.1.1 Synaptic plasticity and neural networks

From the introductory section we assumed that the origin of memory is to be found at the level of the neuron networks. Each neuron may form thousands [5] of synapses with a similar amount of distinct neurons, while the transmission of the information from a neuron goes through a pattern of binary states which are the result of the spatial integration of the excitatory/inhibitory post-synaptic potentials (EPSP or IPSP) on the neurites and the soma [6, 7]. So, determining how a neuron codifies the memory information is not a trivial problem to solve.

An early thoughtful insight into this problem was given in 1949 by the Canadian psychologist Donald Hebb [8]:

> When an axon of cell A is near enough to excite a cell B and repeatedly or persistently takes part in firing it, some growth process or metabolic change takes place in one or both cells such that A 's efficiency, as one of the cells firing B, is increased. The most obvious and I believe much the most probable suggestion concerning the way in which one cell could become more capable of firing another is that synaptic knobs develop and increase the area of contact between the afferent axon and efferent soma.

The so called *Hebb's principle* assumes that a coherent activity[1] between neuron A and neuron B modifies the strength of the A-B connection. The simplest case is that neuron A input contributes hugely to the fire of neuron

[1] From the complex patterns which have been experimentally assessed in the framework of a hebbian synaptic rule–the Spike-Time Dependent Plasticity (STDP) [9]–it could be useful to extend the concept of time-coincidence of the excited state of pre- and post-synaptic towards a more general time-coherence. Moreover, let's just consider the difficulty to attribute a 'pre-before-post' (or the other way round) synaptic activity timing while dealing with a high-frequence input [6].

B: the synapse A-B is thus virtually 'more important' than others and therefore should be distinguished from the other thousands of synapses. As Hebb amazingly spotted, it is now known that this distinction occurs at both a molecular (modification of the channels composition and their conductances [10, 11, 12]) and a structural level (changes in dendritic spines shape [13], increase in the number of direct connections [14]).

The ensemble of the processes which are involved in the modification of the strength of the synapse between two neurons is called *synaptic plasticity*. However, while synaptic plasticity could be considered as an information storage process, it should not be thoroughly assimilated with the common concept of information storage as the writing on a support (e.g. a book, a USB disk) modifying a certain amount of states. In fact, while the information written on a disk can be retrieved through *reading* the encoded data, the biological information memorized as a pattern of modified synapses acts on the global information processing of the neural network [15]. The image of memory recollection as a network information flow could be joined with the theoretical framework of the engrams and the memory traces [2], and thus bridges memory phenomena at the subcellular and moleular level to the cellular and population level [17]. In support to this idea, recent behavioral evidences in mouse show that the optogenetic shrinkage of the facilitation-tagged synaptic spines after a rotarod learning task leads to a task-recall deficit [19].

1.1.2 The molecular systematics of memory

Memory could be generally divided according to two criteria [1]: the time course (long-term[3] or short term memory), and the nature of the stored

[2]Indeed, the exact meaning of the concept of engram, starting from the early definition by the German zoologist Richard W. Semon [16] as

> [...] the enduring though primarily latent modification in the irritable substance produced by stimulus [...],

is not straightforward [17]. For example, after the famous experiments of "false memory creation" using optogenetics by the group of Susumu Tonegawa [18], it has been debated whether the association protocol created a real memory or just an association between a context and a noxious stimulus.

[3]Indeed, long-term memory is itself a phenomenon with a complex time course. A simple (maybe simplistic) division includes a memory *initiation* step, where the synapse undergoes a series of molecular modifications which identify it from the contour synaptic crowd, then a *consolidation* step, which 'embed' the memory information in the synapse molecular machinery (this is a fundamental process, because the disruption of consolidation mechanisms induces an irreversible loss of memory), and the *maintenance* of memory, which is the actual long-term storage of the acquired information. It is important to notice

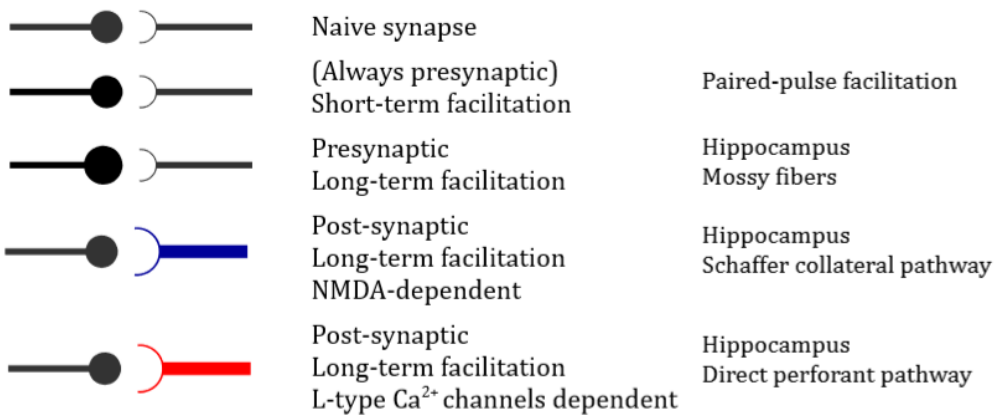

Figure 1.1: An example of molecular systematics of memory processes in the hippocampus. Adapted from [1].

information (declarative or non-declarative). Moreover, from a molecular point of view, the cellular localization (i.e. pre- or postsynaptic) of the plasticity mechanisms should be added as a further classification criterion.

The Figure 1.1 shows part of the multiform ecosystem of memory processes in the hippocampus. It is useful to notice that the same time-scale memory process (Long-term potentiation) can have different cellular localization and underpinning processes.

A caveat on LTP Now it would be the case to discuss some epistemological and experimental issues with the commonly-measured Long-Term Potentiation (LTP). Getting an exponentially growing importance since it was first studied *in vivo* in the early seventies [20, 21], LTP is now in molecular neuroscience of memory a 'do it otherwise referees will ask it' measure for synaptic plasticity. LTP, being a long-term physiological modification at cellular level, has been traditionally considered as *the* point where to search the transition between high-level behavioral memory to low-level molecular memory [20, 22]. This scientific program is reasonable and almost unchallenged [22, 23], however there should be some methodological concern (indeed not commonly applied) while dealing with this topic. Starting from an example: the hippocampus slices from the Brevican *ko* mouse model, when stimulated with a LTP-inducing current injection at the level of CA3, show

that the processes of long-term memory formation are usually *parallel and independent* in respect of learning and short-term memory molecular mechanisms.

an LTP impairment[4] (the impairment is also reproduced by the action of anti-Brevican antibodies in a slice from a wild-type mouse), while the behaving Brevican$^{-/-}$ mouse shows normal memory and learning functions [26]. Let's assume that in [26] there is no experimental bias that would interfere with the LTP formation[5], these results would at least arise a few questions of nontrivial answer. First of all, is the LTP which is induced *ex vivo* the same LTP which is induced *in vivo*? From a very conservative point of view, the fact that hippocampus slices respond to, for example, pharmacological treatments in a similar way compared to behaving animals means that these two forms of synaptic plasticity have some common pathway hubs, but not that they are globally equal. Extending these considerations, the induction of LTP through HFS (High-Frequency Stimulation)–or even using the more physiological [25] *ϑ-burst stimulation*–could be so different compared to the physiological context, that the evoked synaptic plasticity would be an *ad hoc* phenomenon with little or no homolog mechanisms in the active brain. However, such an extreme reasoning does not have a good heuristic value, because there is a great amount of evidences which correlate the dynamics of LTP with behavioral memory [12, 25, 28] and confirm that LTP is a good (but not perfect [25, 29]) *model* for synaptic plasticity and possibly memory phenomena. Last, but not least, the *intrinsic molecular variability*, introduced in Figure 1.1, of the neurophysiological phenomenon LTP is a further and fundamental confounding factor while assessing experimentally the synaptic plasticity. Pojeong Park and colleagues have dissected part of the molecular mechanisms underlying NMDA-depedent LTP and proposed a subdivision in three categories: the *LTPa* (or Short Term Potentiation–STP) which is protein synthesis independent, the protein synthesis resistant *LTPb*, and the PKA- and protein synthesis-dependent *LTPc* [27]. A given high-frequency pattern of stimulation would then elicit one or more forms of NMDA-dependent LTP [27]: it is not known, however, if there are other parallel LTP phenomena in NMDA-dependent plasticity. If this separation is biologically significant, it would explain the fact that in the literature are

[4]The LTP is evaluated considering the slope of the tangent line to the rising EPSP function (a higher response leads to a steeper function, and thus to a higher absolute value of the slope) at different time points, in a time window between one hour (short/middle term potentiation) and four hours [1, 24]. If there is not the stabilization of a given EPSP value between 1 and 4 hours, the LTP is said to be impaired. Please note that the stability of the enhanced EPSP is evaluated *in slice* for an arbitrary and relatively short amount of time: a few hours, while in the animal the LTP lasts at least several months [25].

[5]Actually, this assumption is not banal [27]. In fact, it has been shown that many external factors, such as temperature, age, sex, social isolation, and even the circadian or the estrous cycle of the animal (see [20] for further references) would interfere with the formation of LTP–or rather some forms of the LTP family.

reported cases of long-lasting LTP induced by a single-burst [30], or without protein synthesis [30, 31]. Anyway, the separation of the independent components of LTP will probably help the field to overcome the many experimental controversies which can arise when many superimposed (and sometimes opposite) processes are investigated as if they were a single one.

1.1.3 A general problem for memory maintenance

The main problem when dealing with molecular memory is the fact that the half-life of any molecule (protein or RNA) in the synapse is shorter than the duration of memory–which could last for days, or even a lifetime [32, 33].

Many possible solutions to such a problem have been proposed, from the fancy memory information-encoding through posphorylation of the microtubules[6] [34], to the molecular bistablity [32, 36, 37], and eventually to functional amyloids [12, 33, 38].

Molecular bistability Given a system with two stable states (namely, an active state and an inactive state), the system is bistable when a threshold input would switch the whole system between the two states [32]. Histeresis[7] is a requirement for bistable systems [36], and network motifs such as positive feedback loops (see e.g. BDNF-TrkB [39]) or multi-site phosphorylation (e.g. CaMKII [32, 40]) are prone to show a bistable behavior. Bistability has been predicted in models of CaMKII [32], PKC-MAPK interaction and others [36] and would be a long-term self-sustaining property which could account for the local synaptic long-term modifications[8]. Also, bistability could arise from

[6]It is of notice the model where the CaMKII phosphorilation pattern on a microtubules could function as a memory storage device (more or less like a USB stick) [34]. The modular and stable structure of microtubules have inspired a lot of other mumbo-jumbo theories, whose is mentionable the 'Orchestrated objective reduction' theory by Roger Penrose which claims that consciousness arises from quantum events occurring in neuron microtubues [35].

[7]Histeresis is defined as the time-based dependence of a system's output on present and past inputs.

[8]However, the real picture seems to be a bit more complicated. Let's consider the case of CaMKII. Starting from the experimental and theoretical studies of John Lisman [32, 41], it was showed that CaMKII holoenzyme shows a cooperative activation through self-phosphorylation upon biding with Ca^{2+}-Calmodulin [40]. The self-phosphorylation is the key for the bistability predictions [32] and would virtually last permanently after a significant synaptic input. The use of a CaMKII FRET sensor [42] shows that CaMKII is locally active in the dendritic spine upon synaptic activity, however the activation time is 'only' of one minute–that is the local activation of CaMKII is stable, but not really bistable in a biological context.

trafficking motives in multiple compartments signaling systems, as shown by Upinder Bhalla models [37].

Long-term activity Local translation has been shown to be a fundamental step for the transition from early to long-term memory [1, 43]. This step of local production of proteins–that is, from a network point of view, a modification in the local weights of the interactome or the addition of new nodes–can lead to the presence of plasticity-specific isoforms for various proteins. An intriguing protein is the PKMζ a truncated isoform of the PKC protein. The PKC kinase protein has been shown to be involved in the induction of LTM [1, 44] and presents a N-terminus regulatory domain which self-inhibits the kinase domain unless in presence of the signaling-mediated increase of the secondary messenger diacylglycerol[9] [45]. PKMζ is a constantly-active PKC isoform and it has been found to be linked [10] to LTP maintenance [46].

Functional amyloids As it will be seen in the case of CPEB protein family, another molecular strategy to overcome the protein turnover is the formation of a functional amyloids. An amyloid is an aggregate with peculiar biochemical and biophysical features[11] and thus it shows many properties, such as *thermodynamic stability* [49], steep growth and self-templating action [48]. These features justify the role of amyloid formation in the pathogenesis of a plethora of diseases [49], but also in the increasingly found phenomenon of functional amyloids. A functional amyloid is a protein whose function depends on the features of the amyloid state, for example the thermodynamic stability makes the amyloid *long-lived* (an interesting property for molecular memory) and stable against reactive molecules[12]. Being a functional amyloid very stable and self-templating, it could be a double-edged sword for the cell: for example it could undergo a unrestrained growth process and eventually

[9] A similar regulation step is present, for instance, in the PKA protein–whose activation is downstream the increase of the secondary messenger cAMP.

[10] However, the link between PKMζ and long-term memory is controversial[46], starting from the fact that the PKM$\zeta^{-/-}$ mice do not show a peculiar impairment in long-term memory [47]. That would mean that PKMζ is an important–but not a key–effector of LTM, given that its loss can be compensated by other local network mechanisms.

[11] An amyloid is formed by the interaction of protein segments with a β-sheet conformation in a quaternary cross-β folding: this peculiar structure leads to an amyloid-specific pattern of X-ray diffraction [48].

[12] The human amyloid Pmel17 is a paradigmatic case of functional amyloid [50]. This protein is found in the melanosomes, the organelle where melanin is produced in melanocytes, and forms a self-templating scaffold which guides the formation of melanin and buffers the highly-reactive melanin intermediates–due to the intrinsic stability of the amyloid structure.

damage the cell. So the existence of functional amyloid mechanisms should require a strong compartmentalization (e.g. a vescicle, see note 12) and/or tight regulatory mechanism at the levels of protein translation and half-life.

1.1.4 A tale of a dog and a snail

There are two main categories of unconscious learning. Associative learning is an acquisition of information which requires a comparison between events: during this process the system learns about the relationship between two inputs (classical, or *pavlovian*[13] conditioning), or the relationship of an input to the output of the system (operant conditioning) [52]. Non-associative learning, on the other hand, extrapolates the properties of a single repeated input–for example in case of *habituation* (the input is not important, do not respond), or of *sensitization* (the input is important, respond more promptly) [1, 52].

In the previous paragraphs we assumed that synaptic plasticity (page 5)

[13]The Russian physiologist Ivan Pavlov (1849-1936) studied the 'conditioned reflexes' in dogs.

> The animal can be given food regularly every thirtieth minute, but with the addition, say, of the sound of a metronome a few seconds before the food. The animal is thus stimulated at regular intervals of thirty minutes by a combination of two stimuli, one of which is the time factor and the other the beats of the metronome. In this manner a conditioned reflex is established to a compound stimulus consisting of the sound plus the condition of the hemispheres at the thirtieth minute, when both are reinforced by food. Further, if the sound is now applied not at the thirtieth minute after the preceding feeding, but, say, at the fifth or eighth minute, it entirely fails to produce any alimentary conditioned reflex. If it is applied slightly later it produces some effect; applied at the twentieth minute the effect is greater; at the twenty-fifth minute greater still. At the thirtieth minute the reaction is of course complete. If the sound is never combined with food except when applied at the full interval, in time it ceases to have any effect even at the twenty-ninth minute and will only produce a reaction at the thirtieth minute but then a full reaction. [51]

Conditioned reflexes are now known as classical conditioning. A classical conditioning paradigm is composed of an *unconditioned stimulus* (US), e.g. a little shock, and a *conditioned stimulus* CS+ (a sound, a contextual environment, and so on) which is to be associated to the US, and a control stimulus CS− not associated to the US. To get pavlovian conditioning the CS+ is presented slightly before the US–this process is repeated for a few distanced times. After conditioning, the CS+ stimulus would evoke the same reaction of the US, while the CS− would not. Indeed, classical conditioning undergoes a more general process of evaluation of the correlation between CS+ and US: partially correlated stimuli rise a certain amount of conditioned response, which is proportional to the degree of their correlation [1].

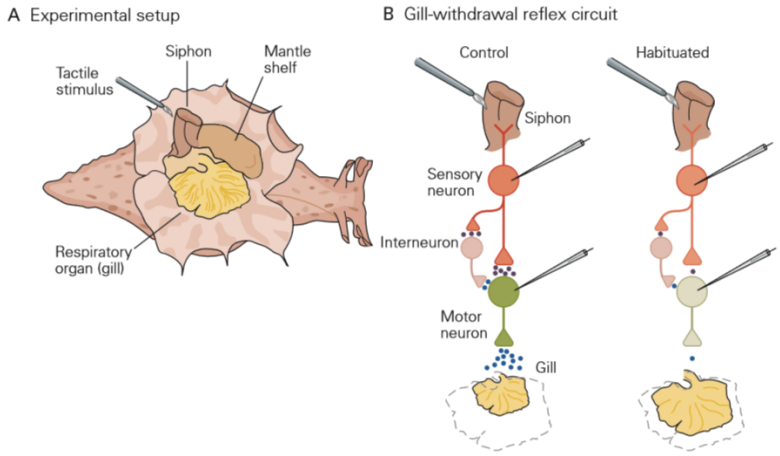

Figure 1.2: A) The gill withdrawal reflex in *Aplysia*. B) Neuronal circuitry underlying the habituation of the gill withdrawal reflex (see text for more information). *From [1].*

is the physical substrate for learning and memory. We thus need an *experimental model*, first to test the association between synaptic plasticity and memory, and then to link the general phenomenon of memory to its underlying molecular mechanisms. Starting from the late Sixties, Eric Kandel began a biological approach to the problem of memory using the sea hare *Aplysia californica*. The advantages of using a lower invertebrate model to dissect a complex phenomenon such as memory is that 1) it is simple[14], 2) it is reliable, because the spatial positions of each neuron type are maintained among different animals, 3) it shows stereotyped behaviors[15], that undergo modification upon experience (a.k.a. learning) which can be retained for a long time (memory). Figure 1.2 shows the mechanism and the circuitry underlying one of these behaviors, the gill withdrawal reflex (see note 15): the sensory neurons (SNs) from the siphon synapses with the motor neurons (MNs) of the gill and with a network of neuromodulatory interneurons. An electric shock from the tail induces a strong stimulation of the serotoninergic interneurons, which induce an *heterosynaptic facilitation* of the SN-MN synapse (conditioned sensitization).

[14]Aplysia brain is an *abdominal ganglion* composed of roughly 20.000 neurons–let's just compare them to the millions of a lower vertebrate brain, such as a frog one. Moreover each ganglion neuron is big, almost visible without magnfication!

[15]One of these behaviors is the *gill withdrawal reflex*: when a stimulus is applied on the siphon, the sea hare withdraws its external gills for a given extent (Figure 1.2 A). This reflex shows habituation: when the same non-noxious stimulus has been presented to the siphon for many times, the gill retraction becomes gradually smaller and smaller (Figure 1.2 B).

The Aplysia system permitted to unravel some of the basal molecular mechanisms underlying synaptic plasticity, which have been confirmed also in insects and in vertebrates[16]. To state a few examples: the role of cAMP rise and the PKA signalling[17] [53], which is necessary and sufficient for the formation of long-term facilitation, the diacylglycerol-mediated signaling of PKC [1, 54], the role of the ubiquitin-proteasome system to target specific proteins (in particular the repressor subunit of PKA) to degradation [55], or the importance of local translation for the consolidation of memory [43]. Experiments using *in vitro* neuronal cell cultures (Figure 1.3), where a single SN forms synapses with two distinct MNs and the heterosynaptic facilitation is induced by some operator-given serotonin puffs, confirmed the synapse-specificity of plasticity mechanisms[18] [1].

1.1.5 An RNA-centric view of memory

Another interesting experimental feature of the *Aplysia* neurons *in vitro* system (see Figure 1.3) is the phenomenon of *synaptic capture*. From the previous paragraph it has been seen that, in order to achieve a long-term facilitation, it is necessary to have a nuclear transcription step–CREB1 and its downstream genes, see note 17–and a subsequent step of emetine- and rapamycin-sensitive [1] local translation[19]. The transcription of new memory-

[16]The molecular processes underlying memory are astonishingly conserved through evolution, even though the major point of synaptic plasticity in invertebrates is the pre-synaptic neuron, while the opposite is true for mammals.

[17]The PKA protein is a heterotetrameric kinase, which is composed of two catalitic subunits which are inhibited by two repressor (R) subunits. Each repressor unit shows two cAMP-binding pockets: when the local cytoplasmic levels of cAMP rise, two cAMP molecules bind the R pockets, thus inducing an allosteric modification and the release of the catalytic units [53]. The R subunits can be also targeted to degradation by specific ubiquitin hydrolases, in order to stably increase the levels of free PKA catalytic units at the synaptic level. The PKA probably has a double function in long-term facilitation: a local increase of active PKA induces the phosphorylation of some focal synaptic targets, such as the *delayed rectifier* K^+ *channels*–the phosphorylated channel is more likely to be closed, so there is a prolonged depolarization state of the pre-synaptic terminus, with a consequent increase of the neurotransmitter release, and *synapsin*, a vescicle protein which induces an increased *docking* of neurotrasmitter vescicles when phosphorylated [1]. PKA is thought to act also as a retrograde messenger: the nuclear translocation of catalytic PKA increases the levels of the immediate early gene CREB1, which is a transcription factor for other Plasticity-Related Products [1].

[18]The long-term facilitation, induced with five puffs of serotonin at the synapse 1, is not extended to a non-stimulated synapse 2. A single puff of serotonin induces only a rapidly decaying facilitation.

[19]Emetine and rapamycin are two inhibitors of protein translation. Emetine acts through its binding to the 40S ribosomal subunit and thus is a complete blocker of transla-

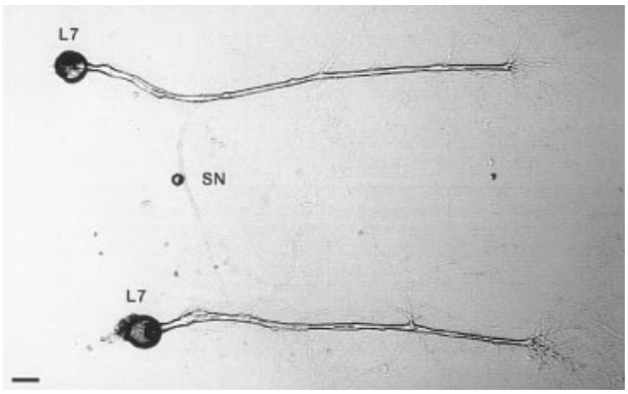

Figure 1.3: Example of bifurcated *Aplysia* sensory neuron (SN), which synapses with two L7 effector motor neurons (MN): this is an *in vitro* system which is indeed suitable to test the synaptic independence of plastic phenomena or the paradigm of synaptic capture. *From [43].*

associated mRNAs could involve the whole cell, so when a specific synapse induces a plasticity process all the other synapses could potentially 'benefit' from it. Indeed, this is what happens during the experiments of synaptic capture: given the system schematized in Figure 1.3, if a strong serotonin facilitation input (5 puffs) is given at one synapse and in the meantime a weak input is given at the other one, both the synapses undergo long-term plastic facilitation [1], even if the 'captured' synapse would show a less marked phenotype.

A powerful conceptual model that explains the general phenomenon of synaptic capture–which is a general *associative property* of the hebbian synapse, even in mammals[20]–is the *synaptic tag and capture hypothesis* [57, 58]. The first enunciation of the model [57] hypothesized that a strong synaptic stimulation induces 1) a *synaptic tag* of the activated synapse and 2) a retrograde signaling which begins the production of 'plasticity related proteins' from the somatic compartment. These proteins would be then 'captured' by the tag and would induce the functional and plastic modifications only of the activated synapse. The phenomenon of synaptic capture would be thus explained by the fact that the weak stimulation induces a tag in the second

tion. Rapamycin acts on particular ribosome-regulating complexes (in mammalian called mTORC–mammalian target of rapamycin complex). So, while emetine blocks both the induction and the consolidation of memory [43], rapamycin is a specific blocker of local translation-mediated memory consolidation [56].

[20]Synaptic capture is a mechanism which occurs also in mammal hippocampus at the level of the CA3-CA1 synapse: a strong stimulation from a Schaffer collateral and a weak stimulation from a parallel one induce LTP in both synapses [1].

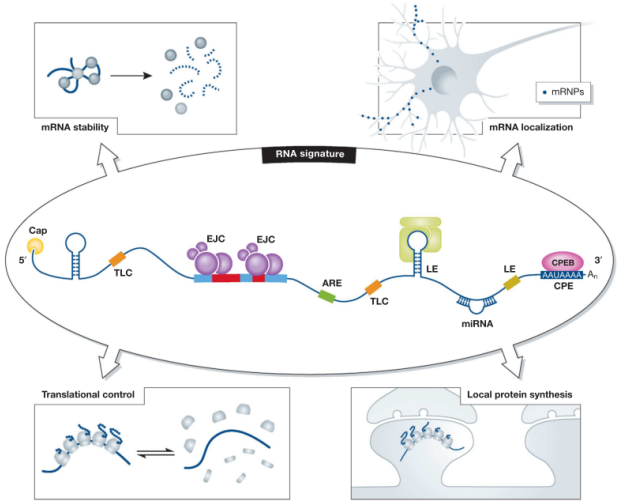

Figure 1.4: The RNA binding proteins are involved in the dendritic transfer of mRNAs, in translation suppression and mRNA stabilization, and in the synaptic activity-dependent mRNA translation. See text for further details. *From [59].*

synapse and both the activated synapses could capture the plasticity related proteins[21] and become facilitated. A subsequent formulation of the hypothesis [58] would change the molecular species underlying the transmission of plasticity information: the 'plasticity related products' are *mRNAs* which would be then captured and locally translated in the tagged synapses.

It has been shown that mRNAs are produced and actively localized in mammalian dendrites after strong synaptic activity [59, 60, 61], and they are likely to be stored in *translation-inhibiting RNA granules* until their translation is again facilitated[22] by synaptic activity [59, 64, 65, 66] (see also Figure 1.4). Different RNA binding proteins (RBPs) interact with the mRNAs

[21] Two main problems arise from the concept of plasticity related proteins. First, the fact that a somatic protein should be directed in some way to the specific dendrite branch and spine, and in any case it would require a big amount of protein to be translated in order to fully cover the dendritic tree. Moreover the tag should act as a spine-specific filter in order to capture with precision the plasticity proteins. Second, plasticity related proteins would not require local translation, so the inhibition of synaptic capture through weak stimulation and the subsequent addition of the translation blocker emetine [43] would not be explained.

[22] The role of RNA binding proteins in these mechanisms of RNA transfer and activity-dependent reguation is indeed fundamental. Just to make an example, the protein FMRP (Fragile-X Mental Retardation Protein), which is fundamental in the pathogenesis of the fragile X syndrome, is an RNA binding protein which is involved in dendritic mRNA transfer and the regulation of translation according to the synaptic-activity [62, 63, 64] .

thanks to the presence (mainly in the uncoded regions of the mRNA) of *in cis* RNA elements called ZIP sequences [59, 66]. So there is a combinatorial effect of the non protein-coding information encoded in the RNA sequence which determines the localization, the half-life, and the timing of translation of the different mRNA species [59].

1.2 The CPEB protein family

The *Cytoplasmic Polyadenylation Element Binding* (CPEB) proteins are a family of evolutionarily conserved[23] (Figure 1.5) ubiquitary RNA binding proteins that are involved in the regulation of the local translation of their target mRNAs [67].

The CPEB proteins have been involved in a plethora of molecular mechanisms, such as embryogenesis, tumor progression, gametogenesis, ageing, cell polarity, and synaptic plasticity [68]. If is of peculiar interest the role of CPEB in gametogenesis [67, 69] and in synaptic plasticity [12, 33, 38, 54, 70, 71], because both these phenomena involve *highly asymmetric cells* (i.e. cells with distinct compartments, such as the distal dendrites, the soma-dendrite and the axon).

1.2.1 Structure and mechanisms

Two major classes of CPEB have been recognized [72]: the *CPEB1-like* class, which includes the homologs of vertebrate CPEB1, and the *CPEB2-like* class, which includes the homologs of vertebrate CPEB2 and its paralogs CPEB3 and CPEB4 (Figure 1.5).

All the CPEB proteins present a similar structure (Figure 1.6): a N-terminus which usually lacks a defined secondary structure, two peculiar RNA binding motives that bind to the target sequence of the RNA (namely, the CPE element) with a precise 3'-5' directionality [68], and a C-terminus folded domain, called ZZ domain, which probably mediates the protein-protein interactions with the translation initiation complex. From a functional point of view, every CPEB protein assumes two states: 1) a *naive*, translation-inhibiting state and 2) an *active*, translation-promoting one. The transition between a state and the other occurs through post-translational modifications, classically the phosphorylation of a threonine residue in the N-terminus [68, 74]–or the novel mechanism of prion-like aggregation and activation found for the neural isoform of *Aplysia* CPEB (*Ap*CPEB, a CPEB1-

[23]The most conserved part of the protein is the RNA binding domain, while the regulatory N-terminus can be wildly different.

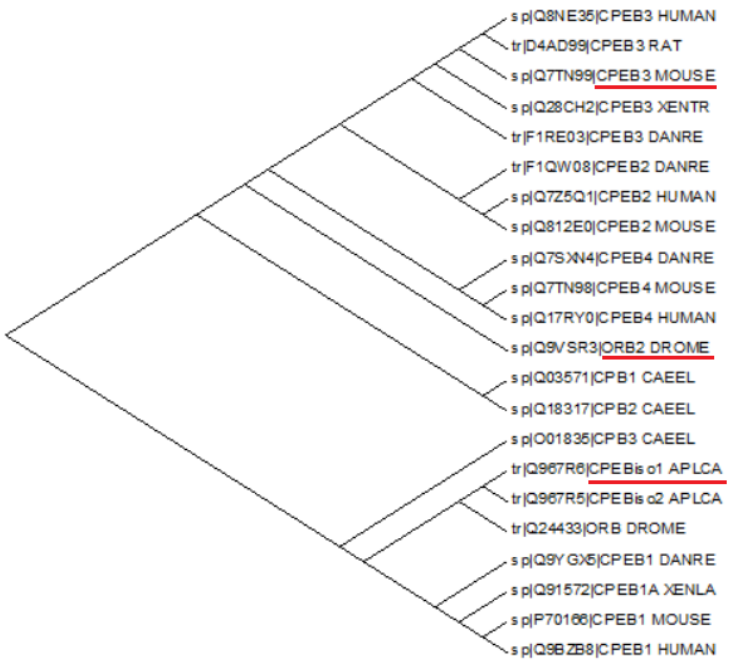

Figure 1.5: Phylogenetic tree (maximum likelihood algorithm) of some members of the CPEB protein family. Two evolutionarily conserved major branches can be spotted: the group of vertebrate CPEB1 hortologs, and the group of CPEB2-like hortologs. The proteins with experimentally demonstrated prion behavior are underlined in red. XENTR: *Xenopus tropicalis*, DANRE: *Danio rerio* (zebrafish), DROME: *Drosophila melanogaster* (fruit fly), CAEEL: *Caenorhabditis elegans*, APLCA: *Aplysia californica*, XENLA: *Xenopus laevis*.

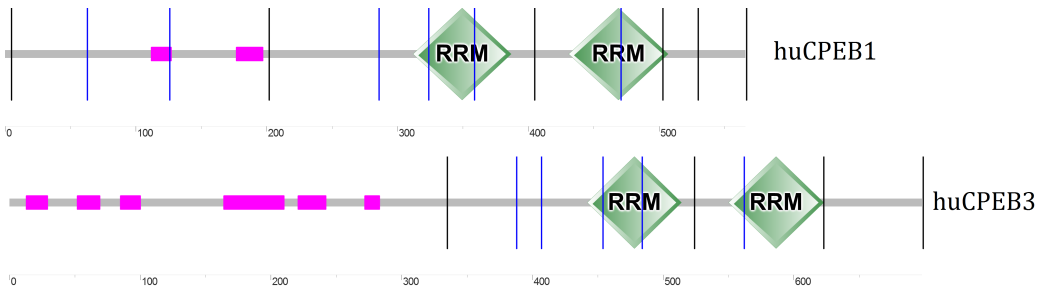

Figure 1.6: Analysis of the structural motives of human CPEB1 and CPEB3 proteins using the SMART algorithm [73]. Pink: low-complexity regions (CPEB1: S-rich regions, CPEB3: polyQ, P/Q-rich and S/L-rich regions), RRM: RNA recognition motif.

like protein) [75], *Drosophila* Orb2 [38] and mouse CPEB3 [76] (two CPEB2-like proteins).

The two classes (CPEB1-like and CPEB2-like) show some mechanistic differences in their function. CPEB1-like proteins, in fact, bind the CPE element on target mRNAs and directly regulate[24] the polyadenylation of the bound mRNA [54, 67, 72], while the CPEB2-like proteins do not regulate directly the length of the poly-A tail of target mRNAs, nor they bind a CPE [72, 77, 78].

1.2.2 *Aplysia* CPEB is a functional prion

The *Ap*CPEB protein has been discovered by the group of Kandel [54] as a local translation regulator, which is induced in a rapamicin-sensitive way by a facilitatory serotonin input and which is downstream the PKA signalling pathway.

The N-terminus of *Ap*CPEB is intrinsically disordered and presents an enrichment in glutamine and asparagine (about the 48% in the first 160 aminoacids) [75]. These features are similar to the prion domains of *yeast prions*, which mediate *dominant cytoplasmic inheritance* in stressful environments[25]. In order to check whether *Ap*CPEB N-terminus could act as a prion there are some peculiar requirements to fulfill [75]: 1) it must be dispensable for the function of *Ap*CPEB (so, ΔN-*Ap*CPEB should be able to bind the mRNA); 2) it should be present in at least two states: a soluble and an insoluble–usually aggregated and amyloid–state; 3) the aggregated state should be self-sustaining (by protein-only dependent conformational modications) and able to propagate its state (cytoplasmic dominance).

Using a β-Gal reporter with a CPE element on its 3'UTR cotransfected with *Ap*CPEB in yeast, Kausik Si and colleagues [75] have shown that the N-terminus does not affect the RNA binding ability of *Ap*CPEB RNA binding

[24]The CPEB1-like proteins influence at least two mechanisms involved in the initiation of translation: the block of mRNA circularization gained through the binding of the CPEB partner *Maskin* to eIF4E, and the poly-A tail polimerization equilibrium between the polymerase *Gld2* and the esonuclease *PARN*. The activation of the CPEB1-like protein would remove Maskin from its site, thus permitting the binding of eIF4G to eIF4E and the circularization of the mRNA, and would take off the PARN esonuclease from the complex, thus permitting the formation of the poly-A tail of the target mRNA.

[25]The dominant cytoplasmic inheritance is a non-Mendelian pattern of inheritance which involves an epigenetic gain of function/loss of function through conformational modification of some cytoplasmic proteins. The modified proteins should be able to self-propagate their state to other naive units, namely they act as prions. This mechanism permits the yeasts to amplify their phenotype variability (useful in stressful environments) without the need to encode the information through genome mutations.

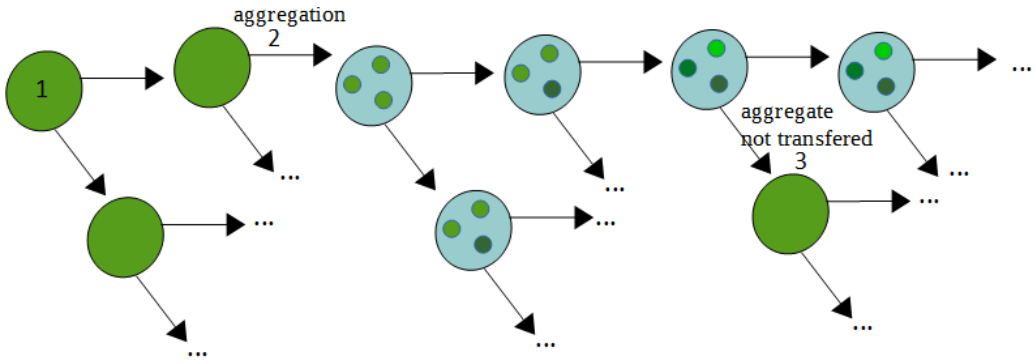

Figure 1.7: *Aplysia* CPEB in a yeast expression system acts as a prion: a GPF-tagged *Ap*CPEB is co-expressed with a βGal-CPE reporter (blue). The naive state of CPEB is translation-inhibiting and diffused (1): this state is passed to the progeny of the yeast cell until N-terminus mediated aggregation occurs (2). The aggregates are transcriptionally active (blue reporter) and can be passed to the progeny: a single parental aggregate mediates the protein-only conversion of the naive *Ap*CPEB in the progeny. The aggregation-mediated gain of function occurs with a rate which is much bigger than what would be expected with random genome mutations(see note 26), and moreover it is reversible (3). Of course the reversibility is a property of the yeast system: the derived 'loss of function' is more likely to have origin in the loss of aggregate inheritance (3) rather than a disaggregation of the amyloid seed.

domain, but its presence induced the metastable translation of the reporter in a 20% of the cotransfected colonies[26] (Figure 1.7). A further characterization of the N-terminus confirms that it occurs in two states (a soluble and an aggregated one), and that the aggregated state is the translation-inducing one [75]. In order to prove the cytoplasmic inheritance of *Ap*CPEB aggregate state, a *cytoduction*[27] experiment has been performed between β-Gal positive

[26]Naive *Ap*CPEB is translation-inhibiting also in the yeast system, however in some colonies there is the functional conversion to a translation-permissive state and thus the reporter is translated. Moreover, a blue colony (β-Gal expressing) has a progeny blue colonies, and sometimes (0.5%) of reverted white colonies, and so on [75]. Indeed, a few colonies (0.005%) which were transfected with N-truncated *Ap*CPEB were transcriptionally active[75].

[27]The cytoduction technique permits to assess the cytoplasmic propagation of the aggregation-prone conformation. The cytoduction exploits the mechanism of yeast sexual reproduction between a donor cell with a nucleus fusion deficit (no genetic exchange) and a trophic selection, and a receiver cell with a mitochondria deficit (so it is unable to grow on non fermenting carbon sources–e.g. glycerol) and a different trophic selection. The mated

*Ap*CPEB donor cells and β-Gal negative *Ap*CPEB receiver cells. Some of the mated cells became β-Gal positive[28], and this result is strictly dependent on the presence of the *Ap*CPEB N-terminus [75].

Some years later the group of Kandel [33] have extended their *ex vivo* study of aggregated *Ap*CPEB. The overexpression of *Ap*CPEB-GFP leads to the formation of fluorescent *puncta*, i.e. aggregates, and this punctiform feature could be extended[29] to endogenous *Ap*CPEB [33]. First they demonstrated that *Ap*CPEB amyloid-like aggregation is a peculiar phenomenon, which is distinct from the polyQ-mediated aggregation[30] or other prion-mediated aggregation. In fact, the overexpression in *Aplysia* neurons of the RNA binding domain (RBD) of *Ap*CPEB linked to a N-terminal polyQ or to others prion-domains does not show the formation of fluorescent puncta–nor does the overexpression of *Ap*CPEB N-terminus linked to another RBP, such as Staufen [33]. However, the trasfection of a chimeric *Ap*CPEB-N-terminus joined to mouse CPEB1 RBD leads to the formation of a punctuate staining[31] [33]. The role of the globular domain in *Ap*CPEB aggregation, suggested by the evidences of a residual transcriptional activation after the expression of a truncated N-terminus *Ap*CPEB in yeast (see note 26), is likely to be evolutionarily conserved in mammalian CPEB3 [76].

Kausik Si and colleagues have demonstrated that *Ap*CPEB forms detergent-resistant amyloid-like fibrils *in vitro*, and that the fluorescent puncta *ex vivo* are reactive to Thioflavin S, a dye which stains protein aggregates of amyloid nature [33]. The amyloid nature of *Ap*CPEB has been confirmed through solid-state NMR by the group of Ann McDermott [82], which have further

receiver cells should exchange the cytoplasm (mitochondria and thus proteins) with the donor cells in order to survive.

[28]The fact that only part of the cytoducted cells are positive confirms that the entity which mediates the cytoplasmic dominance is discrete (i.e. it is an aggregate, see also Figure 1.7).

[29]The study of protein *supersaturation* as a motive force for pathological protein aggregation or unfolded protein stress [79, 80, 81] is an exciting field of study in protein biophysics. Indeed, the overexpression of an aggregation-prone protein induces an increase of the concentration of the protein and probably its concentration-dependent precipitation/aggregation, so when dealing with aggregating or amyloidogenic proteins it is very important to assess the protein behavior in an endogenous expression environment.

[30]This kind of aggregation is linked to many pathological conditions such as Machado-Joseph disease (Ataxin-3) or Huntington's Disease (Htt).

[31]The need of a CPEB RBD to permit the formation of an aggregate could be of some concern, because it has been shown that in yeast the N-terminus of *Ap*CPEB occurs in two dfferent states event if it is linked to the transcriptional activator of the glucocorticoid receptor [75]. However, being the yeast system highly orthogonal compared to *Aplysia* neurons, it probably lacks all the regulatory mechanisms which interfere in the aggregation of the tested proteins.

characterized the biophysics of *Ap*CPEB aggregated. The aggregates appear to be reversible (at least *in vitro*) [82], and more interestingly, the prion domain in the aggregate core appears to fold in a mixed β-strand (major conformation), α-helix and random coil (minor conformations, which are more prone to regulation) [82].

With a split GFP experiment[32], it has been shown that the aggregates are formed through *Ap*CPEB homopolimerization [33]. Moreover, it was seen that the N-truncated form of *Ap*CPEB, while not forming puncta *de novo*, can enter pre-existing aggregates [33]. Using a photoconvertible GFP, Si and colleagues have also shown that the aggregates undergo a slow molecular turnover *ex vivo*[33] and are thus self-sustaining and self-limiting [33]. Then, they demonstrated that the number of the aggregates in the *in vitro* system of the heterosynaptic facilitatory SN-MN synapse increases after stimulation with five puffs of serotonin (a long-term facilitatory input), and that the inhibition of aggregate formation through the injection in the stimulated sensory neurons of anti-aggregated *Ap*CPEB antibodies inhibits the synaptic facilitation at 48h (but not at 24h) [33]. This is the first, and indeed elegant, demonstration of the functional role of *Ap*CPEB oligomers in the long term facilitation of *Aplysia* neurons.

The group of Kandel have proposed a structural mechanism for *Ap*CPEB aggregation which involves the formation of *coiled coil* quaternary structures [84]. A group of site-directed Q→P mutations in the N-terminus of *Ap*CPEB, that would annihilate the coiled-coil propensity of N-*Ap*CPEB (Figure 1.8A) induced the loss of the prion-like aggregation of the protein [84]. The coiled-coil formation has been proposed by Kandel as a general mechanism for the prion-like functional amyloid aggregation [85], however this claim is hard to be extendable to the mammalian isoform CPEB3 (Figure 1.8C),

[32]In a *split GFP* experiment it is tested the interaction between two proteins: each protein of study is fused to the N-terminus or the C-terminus of a fluorescent protein (e.g. C-terminus of CFP and N-terminus of YFP). If an interaction between the two chimeric proteins occurs, the two halves of the fluorescent protein would come close to reconstitute the β-barrel of the sensor, which would eventually become fluorescent. Of course there is a strong dependency on *where* the interaction occurs compared to where the fluorescent domain is linked, and on whether the interaction is not disrupted by the chimerization.

[33]A few important considerations should be made while considering the apparent molecular turnover of *Ap*CPEB amyloid like aggregates. First of all, all these experiments are made with high concentrations of the protein–so the aggregation dynamics could be artefactual, given the high amount of an aggregation-prone protein. Moreover, it is still not clear whether the 'big' aggregates seen in [33] are the real functional aggregate, or rather a superstructure of smaller, functional oligomers. In the latter case, the photoconversion experiment would not demonstrate a turnover of ApCPEB in the functional amyloids, but a different phenomenon of secondary aggregation and disaggregation in conditions of protein overexpression.

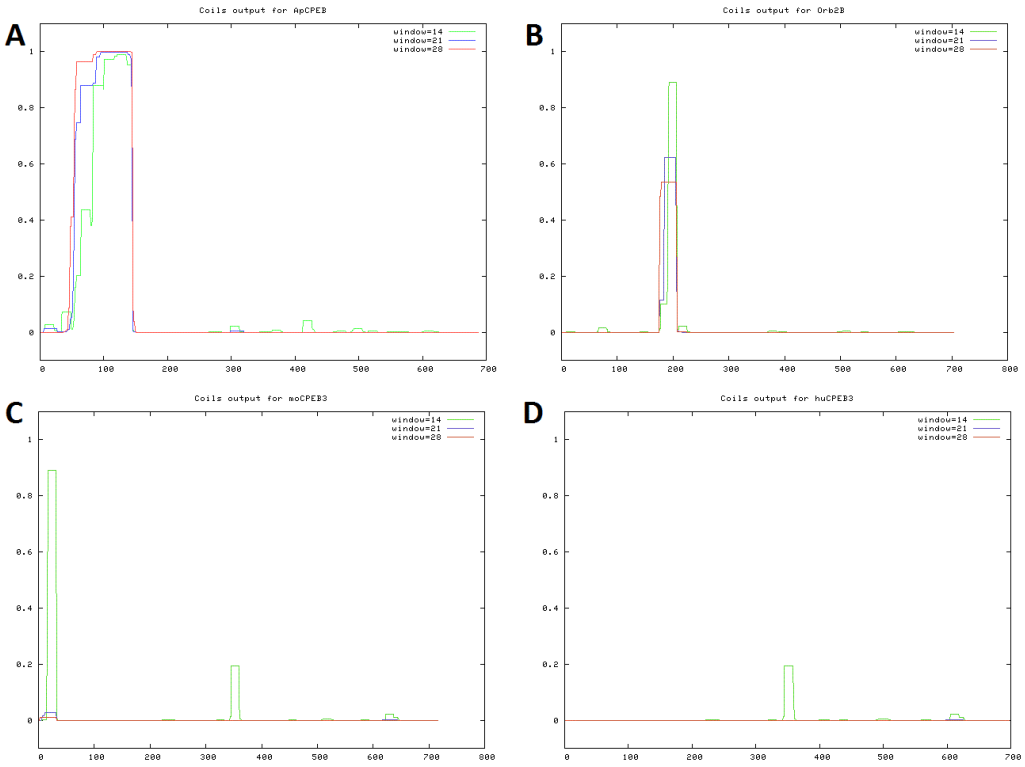

Figure 1.8: Coiled-coil propensity predictions of *Ap*CPEB, Orb2B, moCPEB3 and huCPEB3, using the COIL server (MTIDK, no weighting) [83]. The low coiled-coil propensity of moCPEB3 was consistent after changing the prediction parameters. A window of 28 coiled-coil prone aminoacids (red line) is, from a conservative point of view, the minimum window to consider in order to get a likely prediction of coiled-coils propensity.

which has shown a physiological prion behavior in mice. In fact, similarly to huCPEB3 (Figure 1.6), the moCPEB3 Q-rich N-terminus shows many Proline-Glutamine rich regions which are not prone to significant coiled-coils formation[34].

1.2.3 CPEB2-like *Drosophila* protein Orb2 is a functional prion

Drosophila Orb2 protein, unlike the other fly CPEB protein Orb, shows a prion-prone N-terminus domain [33, 72, 86], which triggers the formation of amyloid-like aggregates that are, again, self-sustainable, self-templating and functionally correlated with LTM [33, 38].

The mushroom bodies and the biology of learning in *Drosophila*

Mushroom bodies (MBs) are a region of insect brain which have been implicated in memory tasks [87, 88, 89] and in multisensory associative integration [90, 91, 92]. They are anatomically composed of a *calix*, more or less extended according to the species, and a peduncle, mainly composed of the axons of the Kenyon cells (KCs), the most abundant intrinsic–i.e. MB-contained–cell type of the MBs. The main circuitry of MBs involves an input from the olfactory glomeruli in the antennal lobe (axons of projection neurons–PN) to the KCs at the calix [87, 88, 92]. Each KC forms synapses with a limited number of PNs (an average of ten [93]), and has typically a very low activity compared to its upstream neurons: this high resistance to excitation makes a KC a strong *coincidence detector* [87, 88] with low levels of noise. KCs receive adjunct inputs from an integrative structure called Lateral Horn[35] and other extrinsic populations, such as dopaminergic and octopaminergic neurons, variously involved in the regulation of learning [88, 92]. KC, then, form synapses with other structures of the brain, called *lobes*, which are divided in five regions (α-, α'-, β-, β'-, and γ-lobes), and whose neurons mediate the motor output from the MBs [89, 92] (Figure 1.9).

MBs have been linked to both olfactory pavlovian conditioning [88] and to the *long-term courtship suppression memory*[36]. In particular, it has been

[34]Interestingly, the N-terminus of moCPEB3 is really similar to the mutated coiled-coil inhibited N-terminus of *Ap*CPEB.

[35]The Lateral Horn input is inhibitory (GABAergic) and probably has a fundamental role in resetting the state of the KC network after the stimulus (the Lateral Horn receives a PN excitatory input) in order to avoid spurious activity [93, 94].

[36]The long-term courtship suppression memory is a peculiar multimodal learning paradigm, where a male fruitfly, previously exposed to a mated, nonreceptive female,

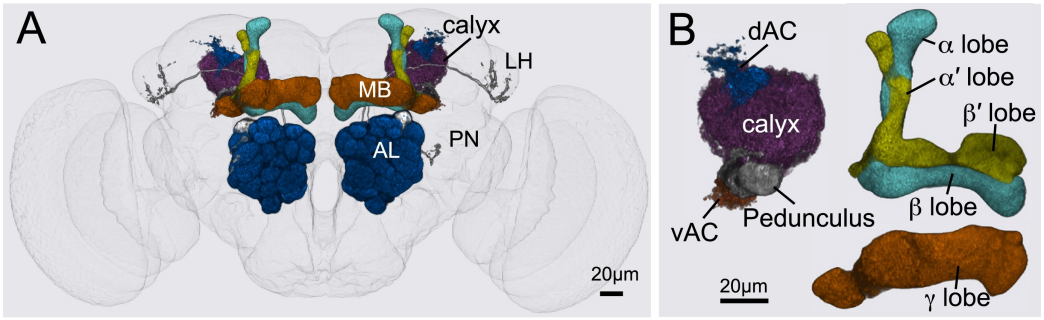

Figure 1.9: Anatomy of *Drosophila* Mushroom Bodies, and of the connected lobe regions. AL: antennal lobe, PN: projection neurons, MB: mushroom body, LH: lateral horn, dAC: dorsal accessory calix, vAC: ventral accessory calix (Kenyon cells to the γ-lobe). *From [92].*

shown that the pherormone signaling which mediated courtship learning involved the activity of a group of dopaminergic neurons towards the DR1 receptors of γ-lobe neurons [91]. Another molecular process which has been found to be fundamental for MB-based learning is the rise of secondary messenger cAMP, which occurs in KC after an optopamine, a dopamine, or an odor stimulus [88]. In order to get an olfactory conditioning the odor stimulus should occur *before* the octopamine/monoamine stimulation [88], but at the same time there are strong evidences for plasticity to occur at the KC axon bouton [88]. Indeed, there is an important spatial problem involved here, because while the octopaminergic stimulation occurs at the calix level, the distance of the facilitation site (that is, the KC axon terminus) is not sustainable by the simple diffusion of, for instance, cAMP [88].

A tight regulation of Orb2 aggregation

A fundamental difference with the *Ap*CPEB system is that the *orb2* gene undergoes alternative splicing and many Orb2 isoforms are produced [72]–of these, two proteins of interest are the isoform A (Orb2A) and B (Orb2B) [33, 72, 86] (Figure 1.10 C). In particular, Orb2B is the most abundant isoform in the cell, is widely diffused and shows no or little aggregation propensity, while Orb2A is little expressed, is locally translated and aggregates quickly in proteinase- and SDS-resistant puncta [33]. It has been shown that Orb2A mediates the local aggregation of Orb2B after synaptic stimulation, thus

learns to inhibit its courtship behavioral program when exposed again to a mated female–but not when exposed to a virgin one [72].

forming a heteromeric[37] Orb2 aggregate [33, 86].

The aggregation propensity of Orb2A makes this isoform a potential burden for the cell proteostasis and thus the Orb2A local level is strictly regulated by the cell through a finely-tuned translation-degradation equilibrium [95]. Indeed, the half-life of the Orb2A isoform is short[38] (about 1.2 hours) However, the activity-mediated binding of Orb2 with its partner[39] *Tob* stabilizes Orb2A, through the interaction of the complex with the Lim kinase, a protein which is translated locally at the synapse after synaptic activity [95]. It is reasonable to believe that phospho-Orb2A, being more stable than naive Orb2A, can accumulate after a significant synaptic stimulation and thus it would be able to undergo its prion-like conformational modification and to aggregate.

A further level of regulation of Orb2A occurs at the mRNA level. The group of Kausik Si has noticed that the Orb2A mRNA occurs in two distinct species: an intron-retaining non protein-coding mRNA, and a mature protein coding (pc) mRNA [97]. There are evidences for a local splicing[40] of the non protein-coding mRNA after synaptic activity, and this process seems to be mediated by the protein NOVA [97].

Orb2 aggregates and long-term memory

Orb2 aggregates have been directly linked to long-term memory. A mutant Orb2A isoform (F5Y) shows defects in Orb2A amyloid-like oligomerization and Orb2 aggregation [38]. Mutant $orb2^{F5Y/F5Y}$ flies show impaired courtship learning and olfactory avoidance long-term memories [38]. The two Orb2 isoforms have complementary roles in LTM-related tasks. In fact, *Drosophila* mutants with a defective Orb2B RNA-binding domain (RBD) show no LTM–when Orb2A RBD mutants show normal LTM [86]. On the contrary, Orb2A Q-rich N-domain is significantly involved in LTM, while Orb2B prion-like domain is not [86]–yet a residual LTM is present in Orb2A IDD-deleted fly mutants, suggesting a minor role for activity-dependent Orb2B homomeric aggregation in Orb2 aggregate formation. In a way, the Orb2 sys-

[37] This is a nice mechanistic homology with the *Ap*CPEB system: a N-terminus truncated form of *Ap*CPEB can enter pre-existing aggregates and recombine the splitted GFP (see note 32) [33].

[38] The half-life assay of Orb2 isoforms has been done with an *in vitro* proteolysis assay using the protein translation blocker cycloheximide and subsequent western blot [95].

[39] Interestingly, also the mouse holomolog of Tob (Tob1) is an interactor of mouse CPEB3 [95, 96].

[40] Interestingly, the mammalian CPEB3 mRNA retains a ribozime sequence which has been shown to self-cleave itself [98], and the self-cleaving propensity has been shown to be important for episodic memory in humans [70].

tem suggests that the underlying processes of the prion-like aggregation in *Ap*CPEB (and in mouse CPEB3) are functionally separated.

It has been shown that the Orb2 aggregation occurs downstream the activation of the dopamine DRD1-type receptor [71], which would likely increase the local concentration of cAMP and the PKA activity. It is nice to notice the fact that the DRD1 signaling in γ lobe neurons has been previously involved in pherormone-mediated courtship learning in *Drosophila* [91]. It has been shown that, after the IDD-mediated aggregation of Orb2(B), the protein aggregate interaction surface changes, and Orb2 becomes a bad interactor of the translation-inhibiting protein CG13928, while gaining affinity[41] towards the translation-promoting partner CG4612 [100]. The released mRNAs could then be involved in synaptic facilitation via multiple parallel processes: many mRNAs which are supposed to interact with Orb2 are involved in synaptic growth and functions [78]. So a single aggregation event could regulate the dynamics of the local proteome (and thus interactome) simultaneously at the level of many network nodes, potentially providing a significant long-lasting change in the local properties of the synapse.

Is Orb2 pre-synaptic or post-synaptic?

The complexity to coherently join the molecular cues for learning, and the structural circuitry of mushroom body could be simplified by the Orb2 system. First of all, Orb2 is expressed in the Kenyon cells [38], and in this region of MBs the protein can be both pre- and post-synaptic [71, 101]. The functional aggregation of Orb2 occurs in a discrete time window[42], and an Orb2 aggregate would be probably localized in a specific branch of the KC axon. So, when dealing with the olfactory aversion conditioning, which involves the activation of a population of dopaminergic neurons innervating the α/β and α'/β' neurons [88, 102], together with the inhibition of γ lobe neurons [103], Orb2 could be the missing link between 1) the cAMP[43] rise in KC, and the likely production of PRPs which can later be 'captured' and translated by the Orb2 aggregate, 2) the odour-specific elaboration of the learned inputs, without the need of multiple parallel groups of KC carrying the same information to distinct regions of the lobes, which would require a facilitation at the PN-KC synapse to diminish the amount of needed KC

[41] The idea that amyloid-like aggregates can become new hubs of local interaction network is not new in the field of protein aggregation studies [99].

[42] As it will be seen in Chapter 4, it is reasonable to suppose that the functional amyloid aggregation acts as an *intrinsic time integrator* through a minutes-wide time window.

[43] A suspicious parallelism with *Aplysia* system would suggest a cAMP-PKA-CREB mediated pathway in KC [104].

cell types, 3) some evidences of pre-synaptic facilitation in olfactory aversion learning paradigms [88].

When dealing with the courtship learning memory problem, however, Orb2 is interestingly required in γ lobe neurons [72]. The courtship learning deficit of the $orb2^{-/-}$ fruitfly is rescued by the expression of Orb2 in γ neurons, but not in α/β or α'/β' neurons [72]. Given that the Orb2A isoform–which is necessary for Orb2 aggregation–has been found in the post-synaptic compartment of the γ lobe neurons[44] [71], it can be stated that in courtship avoidance learning there is a great importance for post-synaptic local translation. Moreover, the post-synaptic Orb2 system would guarantee a strong specificity of the elicited γ lobe output response, even if a single γ neuron would reasonably synapse with a lot of different KCs–which would be activated by many different odorants thus meaning a lot of potential noise[45].

1.2.4 Perspectives: functional prions in mammals

The functional prion-like aggregation is not an exclusive phenomenon for invertebrate brains. Indeed, it has been recently demonstrated that the mouse protein CPEB3, a mammalian CPEB2-like isoform, shows a functional amyloid behavior [76, 105] that correlates with *in vitro*, *ex vivo* and *in vivo* long-term plasticity [12].

Mouse CPEB3 shows a glutamine-rich N-terminus, which is however more complex compared to Orb2A or *Ap*CPEB ones (Figure 1.10 A): there are a Q-rich region (aa 1-33) close to a Q/P-rich region (aa 33-103, see page 34), a regulatory region (aa 128-284) which shows S-rich, Q/P-rich, and S/A-rich regions with a certain propensity to form α-helix secondary structures, and a long unstructured α-helix prone region (aa 285-449) [76]. The use of progressive N-truncated isoforms determined the role of the different portions of CPEB3 N-terminus (Figure 1.10 B), in particular the first 127 amino acids (high-Q percentage) are necessary for the aggregate seeding, but not sufficient for the aggregate cytoplasmic inheritance, aa 128-284 are involved in the regulation of the aggregate and its localization, and aa 285-449 are

[44]Indeed, Orb2A has been found also at the active zones of KCs [38, 71], but the pre-synaptic contibution, while being probably fundamental for olfaction avoidance memory–which is influenced by Orb2 expression [38], seems to be less important for the courtship avoidance memory, maybe because the courtship avoidance is a multi-modal learning task [72, 91]. The only partial dependence of courtship avoidance learning and memory from olfaction stimuli has a neuroanatomical substrate in the probably multimodal inputs from the ventral accessory calix (Figure 1.9) to the γ lobe [92].

[45]However, it should be always kept in mind the important role of *neural network modules* [92] in regulating the properties of the MB system, such as signal-to-noise ratio and others, as it can be seen through neural networks modeling [94].

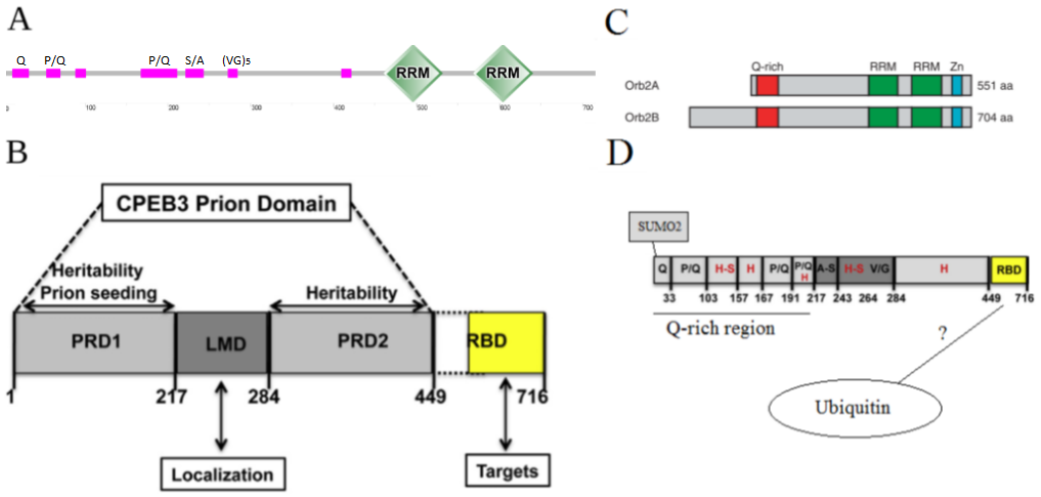

Figure 1.10: A) SMART scheme of mouse CPEB3: low complexity regions and most abundant aminoacid are shown in fucsia. RRM: CPEB RNA Recognition Motif. B) Scheme of moCPEB3 N-terminus domain sub-characterization. *From [76].* C) Scheme of the two isoforms of Orb2 protein. *From [72].* D) The main post-translational modifications of CPEB3 protein (in particular SUMOylation) make it suspiciously similar to the Orb2A-Orb2B system.

involved in cytoplasmic inheritance[46] [76]. Interestingly, there seems to be a probable role for the globular RBD of CPEB3 in its prion-like function[47] [76]. Moreover, Stephan and colleagues have found that the CPEB3 aggregation need the presence of polymerized actin[48], and that there is a positive feedback loop between CPEB3 aggregation and CPEB3-dependent actin mRNA local translation [76].

Dendritic CPEB3 translation has been associated to neuron stimulation *in vitro*, to LTP induction *in slice*, and to the behavioral Morris water maze test *in vivo* [12]. A high increase of CPEB3 oligomerization has been shown to occur *in vivo* after a contextual fear conditioning, compared to the control mice [12]. The group of Eric Kandel has also found that conditional knock-

[46]These residues are probably rich in α-helix secondary structures, so it is possible that they could form *non canonical* coiled-coil loops [106], which would mediate the inheritance of the conformational change.

[47]This was seen with progressive C-truncated CPEB3 constructs expressed in yeast, and it is coherent with the specificity of *Ap*CPEB N-terminus aggregation only when linked to the RBDs of CPEB family which was found in *Aplysia* [33].

[48]The treatment of CPEB3-expressing yeast cells with the actin depolymerizing drug latrunculin A determined the non-formation of CPEB3 aggregates [76].

out mice for CPEB3 show an impaired hippocampal function[49], which can be rescued through restoring CPEB3, but not N-truncated CPEB3 [12].

A companion paper from Drisaldi and colleagues shows that the naive CPEB3 pool is post-translationally modified through SUMOylation [105]. SUMO-CPEB3 is soluble[50] in the cellular context, and forms only small-sized detergent-resistant aggregates *in vitro*, compared to a normal CPEB3 solution [105]. The SUMOylation level of CPEB3 decreases after synaptic activity, thus probably causing CPEB3 aggregation, however the SUMO2 protein is itself regulated by CPEB3 so a negative feedback loop seems to self-regulate CPEB3 aggregation [105]. The structural similarity that a SUMO-N-CPEB3 protein has with the Orb2B protein isoform (Figure 1.10 C and D) is noticeable, so it could be reasonable to suppose that CPEB3 would form the amyloid aggregation seed, while SUMO-CPEB3 aggregates transiently through CPEB3*/SUMO-CPEB3 interactions. Strikingly, it has been shown that CPEB3 aggregates are not long-lived (compared to *Ap*CPEB and Orb2 ones), but there are evidences for the maintenance of a highly stable aggregation seed [12].

The discovery of an evolutionarily conserved prion-like behavior of CPEB proteins opens a lot of exciting possibilities both at the level of basic biology of the neuron[51] and of pathology. From the study of how a neuron can handle a dangerous, albeit functional, molecular entity such as an amyloid, a deeper understanding on the molecular mechanisms of protein aggregation and new strategies to treat pathological amyloidosis would surely arise in the future.

[49]For example, it is known that CPEB3 regulates the activity dependent translation of GluA1 and GluA2 subunits of AMPA receptors [12, 77].

[50]Interestingly, SUMOylation is a conserved process of solubilization for aggregation-prone and amyloidogenic proteins, such as Ataxin3 [107].

[51]For instance, prion-like aggregation could be able to reconcile many different hypotheses for memory formation, such as the synaptic re-entry reinforcement hypothesis or the synaptic tag and capture hypothesis [71].

Chapter 2

The protein aggregation-dependent plasticity model

2.1 Self-sustaining protein aggregation general model

Let's now consider a general equation of local monomer production (the limiting species being in this case Orb2A) which includes the functions of local translation and local degradation:

$$\left(\frac{\partial[M]}{\partial t}\right)_{\text{production}} = k_{tr}(\vec{r},t)\,\rho(\vec{r},t) - k_{deg}(\vec{r},t)\,[M](\vec{r},t) \tag{2.1}$$

where the $k_{tr}(\vec{r},t)$ function describes the translation rate in space and time, $k_{deg}(\vec{r},t)$ the degradation rate, $\rho(\vec{r},t)$ the local amount of Orb2A mRNA and $[M](\vec{r},t)$ the local concentration of the monomeric protein.

Let's now add a dependency of the monomer concentration on the synaptic activity. I assume that the monomer is produced locally after the synaptic stimulus, according to a function of the synaptic stimulus itself:

$$\left(\frac{\partial[M]}{\partial t}\right)_{\text{production}} = k_{tr}(\vec{r},t,\sigma)\,\rho(\vec{r},t) \;-\; k_{deg}(\vec{r},\sigma,t)\,[M](\vec{r},t). \tag{2.2}$$

where σ is the synaptic stimulation time course.

The protein monomer is thus accumulated in a certain time window, which is governed by the parameters of the $\sigma(t)$ function. The accumulation favors the transition to an aggregation-active state, that for Orb2 could

be the formation of an Orb2A oligomeric nucleation seed and for ApCPEB could consist in the transition to the prion-like state. It is reasonable to assume that, in the cell, these molecular mechanisms are strictly regulated in a synaptic-activity dependent fashion: Orb2A is stabilized by interaction proteins like Tob and LimK [95] and it is possible that ApCPEB prion transition is locally regulated by synaptic activity-activated proteins (such as chaperones).

$$\frac{\partial[M^*]}{\partial t} = k_{conv}(\vec{r},t,\sigma)\,[M](\vec{r},t,\sigma) \;-\; k_{deconv}(\vec{r},t,\sigma)\,[M^*](\vec{r},t) \tag{2.3}$$

where the $k_{conv}(\vec{r},t)$ function describes the activation rate evolution, $k_{deg}(\vec{r},t)$ describes the rate of exit from the aggregation-prone state and $[M^*](\vec{r},t)$ is defined as the concentration of monomer molecules that are in the aggregation-prone state.

When a certain amount of monomer protein enters the aggregation-prone state, it is likely that this seed catalyzes the prion-like conversion and thus the aggregation of more monomers:

$$\frac{\partial[O]}{\partial t} = k_{agg}(\vec{r},t,[M^*])\,[M^*](\vec{r},t,\sigma) \;-\; k_{tur}(\vec{r},t,\sigma)\,[O](\vec{r},t) \tag{2.4}$$

where [O] is the amount of monomers in aggregated state–regardless whether they form many short polymers, or few long ones, k_{agg} is the rate of aggregation and k_{tur} is the aggregate turnover rate. It is also plausible that the prion-like conversion rate is a function of the aggregation state $k_{conv} = k_{conv}(...,[O])$.

It has been shown that the size of ApCPEB aggregates in *Aplysia* cells is kept quite constant [33], suggesting that there are mechanisms regulating locally the aggregation efficiency and providing a feedback mechanism limiting the size and number of aggregates to a maximum. It is reasonable to extend this reasoning to other functional aggregates. This would be due to aggregate-dependent changes in the disgregation functions so that $k_{tur} = k_{tur}(...,[O])$, and/or in the levels of free monomer itself ($[M] = [M](...,[O])$) – in the case of Orb2 aggregate. This is plausible because Orb2 RBP regulates also its own mRNA [78].

It is now possible to write the general equations which describe the dynamics of a self-sustaining and self-limiting protein aggregate:

$$\begin{aligned}\frac{\partial[M]}{\partial t} &= k_{tr}(\vec{r},t,\sigma)\,\rho(\vec{r},t) \;-\; k_{deg}(\vec{r},\sigma,t)\,[M](\vec{r},t) \\ -k_{conv}(\vec{r},t,\sigma,[O])\,[M](\vec{r},t,\sigma) &\;+\; k_{deconv}(\vec{r},t,\sigma)\,[M^*](\vec{r},t)\end{aligned} \tag{2.5}$$

$$\frac{\partial[M^*]}{\partial t} = k_{conv}(\vec{r},t,\sigma,[O])\,[M](\vec{r},t,\sigma) \;-\; k_{deconv}(\vec{r},t,\sigma)\,[M^*](\vec{r},t) \\ -k_{agg}(\vec{r},t,[M^*])\,[M^*](\vec{r},t,\sigma) \;+\; k_{tur}(\vec{r},t,\sigma)\,[O](\vec{r},t) \tag{2.6}$$

$$\frac{\partial[O]}{\partial t} = k_{agg}(\vec{r},t,[M^*])\,[M^*](\vec{r},t,\sigma) \;-\; k_{tur}(\vec{r},t,\sigma)\,[O](\vec{r},t) \tag{2.7}$$

The aggregate [O] is the main output of the system, which affects the synaptic efficiency through the regulation of the local translation.

2.2 Protein-aggregation dependent synaptic rule (Orb2-inspired)

In order to model, in a first approximation, Orb2 aggregation I assume a series of conditions, starting from the previous general model. The first one is to consider the synapse as a punctiform compartment neglecting space variables and that there is no diffusion of the Orb2A protein outside the synapse. The second assumption is that the number of Orb2A mRNA molecules locally available for translation are constant; this is justified by growing evidence about a Orb2A mRNA post-transcriptional transition from a somatic non-protein coding to a local protein-coding form, which likely occurs at stimulated synapses thanks to the splicing mediator Nova [97]. From these conditions it comes that the studied variables are only functions of time and their variation is a total derivative according to t. The third hypothesis is that the aggregation seed is composed of Orb2A oligomers [71, 86, 95], while the Orb2 mature aggregate is composed of the Orb2B isoform and, once formed, is completely self-sustaining. So, in the Orb2-inspired model, Equations 2.5 and 2.6 are not linked through the conservation of the monomer species. In partial accordance with Equation 2.6, I assume an (indirect) cross-dependence between the levels of oligomeric Orb2A and Orb2B aggregate. Again, I am considering the aggregate form to be a general state of the protein, without considering the number and/or the size of each individual aggregate. A fundamental assumption for the Orb2 model is that the Orb2A oligomer forms a seed for the further Orb2B aggregation [38, 71, 86, 95] and that–once Orb2 aggregate is grown to a certain level–the Orb2 oligomer becomes self-sustaining and invariant to the Orb2A seed presence. The Orb2A oligomer is thus possibly a synaptic tag to commit the activated synapse to long-term facilitation [71]. Interestingly, a monoaminergic secondary activity is needed for the further consolidation of memory [71, 91] (i.e. in the Orb2 system, the Orb2B isoform aggregation).

Let's assume that the local translation of Orb2A depends on the synaptic activity, according to the following equation:

$$\frac{\mathrm{d}f(\sigma,t)}{\mathrm{d}t} = k_{\mathrm{on}}\,\sigma(t) - k_{\mathrm{off}}\,f(\sigma,t) \tag{2.8}$$

thus, the system response to the synaptic activity (in this case modeled as a binary function $\sigma(t)$, which could be associated with the ON state of a minimum amount of the local monoamine channel population) grows with a k_{on} constant and becomes saturated and unresponsive with a k_{off} rate. The local levels of Orb2A monomer increase after synaptic activity [38, 95] and this growth is regulated by the stabilizing effect of Tob/LimK-mediated phosphorylation of Orb2A and by the destabilization of phosphorylated Orb2A interacting protein Tob [95]: the superposition of these processes likely identifies a time window for synaptic accumulation and oligomerization of Orb2A. Also, if Orb2A is to be considered a synaptic tag, it is likely that the Orb2A production should become insensitive to further synaptic activity after the long-term consolidation of memory–or the formation of Orb2B amyloid-like oligomer which potentially ensures an indefinitely long-lived synaptic facilitation.

The Equation 2.9 tries to include the described properties of Orb2A translation:

$$\frac{\mathrm{d}[A]}{\mathrm{d}t} = \alpha_{\mathrm{tr}}\,[\rho]_A\,f(\sigma,t)\,\Theta_{B^*}^{1\to 0} - \alpha_{\mathrm{deg}}\,[A] \tag{2.9}$$

where α_{tr} is the local translation rate of Orb2A, $[\rho]_A$ is the concentration of Orb2A mRNA–assumed to be constant, α_{deg} is the local degradation rate and $\Theta_{B^*}^{1\to 0}(B^*)$ is a Heaviside-like continuous function which assumes values close to zero when the amount of Orb2 aggregate approaches a threshold value $[B]_{\theta,A}$ and close to one for smaller values.

Orb2A has a strong intrinsic tendency to aggregation [38], so I ignore the transition to an aggregation prone state of the monomer (Equation 2.3) and directly model the Orb2A aggregation:

$$\frac{\mathrm{d}[A^*]}{\mathrm{d}t} = \alpha_{\mathrm{agg}}\,[A] - \alpha_{\mathrm{ex}}\,[A^*] \tag{2.10}$$

where α_{agg} is the aggregation rate and α_{ex} is the aggregate exit rate. Applying the conservation of Orb2A species to Equations 2.9 and 2.10, I obtain:

$$\frac{\mathrm{d}[A]}{\mathrm{d}t} = \alpha_{\mathrm{tr}}\,[\rho]_A\,f(\sigma,t)\,\Theta_{B^*}^{1\to 0} - \alpha_{\mathrm{deg}}\,[A] - \alpha_{\mathrm{agg}}\,[A] + \alpha_{\mathrm{ex}}\,[A^*] \tag{2.11}$$

The Orb2A/Orb2B hetero-oligomerization, which initiates the formation of Orb2 aggregates that correlate with long-term memory, depends on both

the presence of an Orb2A aggregation seed [38, 86] (i.e. oligomer) and of synaptic stimulation [71]. Given that the translation-dependent L-LTM is not induced by an intensive (i.e. non-spaced) training [108] and that *Drosophila* Orb2-dependent LTM easily occurs after a series of stimulations and recoveries [72], a good candidate for this synaptic activity is the hour-long rhythmic dopaminergic stimulation seen by Plaais and colleagues after spaced learning [109], which has been shown to inhibit anesthesia-resistant memory (ARM) and thus to gate LTM [109]. It has been shown–at least for *Aplysia* CPEB amyloid-like aggregates–that the dimensions of the higher-order aggregates (also called *puncta*) are kept at a steady level [33], with a turnover rate of about 20% in 48h. This steady-state behavior could be applied also to Orb2. Also, Orb2 aggregate self-sustaining steady state appears to be independent of the presence of Orb2A–after reaching the mature state. In order to model this complex behavior, I consider a first simplification: both the mRNA and the protein of Orb2B are present at high levels in the cytoplasm, so I assume the translated non-aggregated Orb2B isoform is kept constant at the dendrite level, because the local levels of the protein are instantaneously buffered against a much larger somatic reservoir.

The proposed equation for Orb2B aggregation is the following:

$$\frac{\mathrm{d}[B^*]}{\mathrm{d}t} = \beta_{\mathrm{agg}}\, g(\sigma, t)\, \Theta_{A^*}^{0\to 1}\, \Theta_{B^*}^{1\to 0} + \beta_{\mathrm{ex}}\, (\Theta_{B^*}^{0\to 1} - 1)\, [B] \tag{2.12}$$

where [B]* is the amount of Orb2B in aggregated state, β_{agg} is the Orb2A seed-dependent aggregation rate and includes the (constant) Orb2B monomer level, β_{ex} rules the aggregate dissociation when the oligomer does not reach the steady level and g(σ) is the synapse reaction to a (binary) synaptic stimulation. $\Theta_{B^*}^{1\to 0}(B^*)$ is a Heaviside-like continuous function which assumes values close to zero when the amount of Orb2 aggregate approaches a threshold value $[B]_{\theta,BA}$ and close to one for smaller values: that is, the growth of Orb2B aggregate becomes independent to Orb2A seed after reaching a threshold value. An analogous behavior, but opposite, is true for $\Theta_{B^*}^{0\to 1}(B^*)$ (self-sustaining steady state at $[B^*]_{\theta,BB}$) and $\Theta_{A^*}^{0\to 1}(A^*)$ (responsiveness to the Orb2A oligomer $[A^*]_{\theta,min}$). The Equation 2.12 does not take into account the possible weak homoinduced Orb2B aggregation, which has been hypothesized in order to explain the residual LTM observed in Orb2A-only defective flies [86]. Since it is not been established which are the stimulation dependent parameters of functions f(σ) and g(σ), let's assume that $f(\sigma) = g(\sigma)$ and that Orb2A and Orb2B are both responsive to the same dopaminergic stimulus $\sigma(t)$.

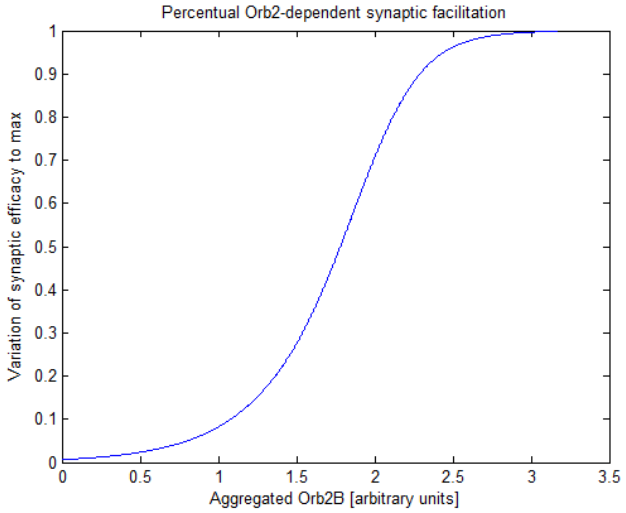

Figure 2.1: Plot of synaptic efficiency variation (% ratio to $\Delta\varepsilon_{max}$) according to aggregate Orb2B concentration (arbitrary units). a=5, b=2.

2.3 Facilitation rule

The PADP synaptic rule states that the synaptic efficiency scales with the amount of Orb2B aggregate; as I modeled the aggregation, after reaching an activity-dependent threshold the aggregate self-templates itself. These conditions imply an all-or-nothing response of the synapse: if a salient condition has been presented for enough time to trigger the formation of an amyloid aggregate, after a reasonable time interval between the aggregation and the consequent translational activation of pro-plasticity factors (called here *latency time* τ), the synapse will make a transition to a higher efficiency stable state. I modeled the PADP synaptic efficiency update with a sigmoidal function (**Figure 2.1**) because it has a steep upper-bounded behavior that is well-suited for the postulated almost two-state plasticity rule,

$$\Delta\varepsilon(t) = \frac{\Delta\varepsilon_{max}}{\sqrt{1 + e^{-a\,(B^*_\tau - b)}}} \tag{2.13}$$

where $\Delta\varepsilon_{max}$ is the maximal ΔEPSP (Excitatory Post-synaptic Potential) found at the synapse after an experimental facilitation protocol, a, b and c are the parameters that regulate the sigmoid function behavior, B^*_τ is the composed function $[B^*] \circ T$ where

$$T : \; t \in \mathbb{R} \longrightarrow t - \tau \in \mathbb{R} \; . \tag{2.14}$$

In this way, also the latency time between the aggregation trigger and the facilitation onset is taken into account.

Chapter 3

Simulation of ordinary differential equations using Simulink®

Given a system of first-order ordinary differential equations (ODEs), the analytic solution is often not available, so the numerical approach is the best choice to get an approximation of the solving solution. Simulink® is an environment for graphical programming developed by MathWorks®, which can be used to easily analyze and simulate dynamical systems.

An example of first-order ordinary differential equation is an equation of the form

$$\frac{\mathrm{d}f(t)}{\mathrm{d}t} = a(t) \cdot f(t) + b(t) \tag{3.1}$$

(it could be easily seen that this equation is similar to the Equation 2.8). A Simulink®block programming of Equation 3.1 is like the following

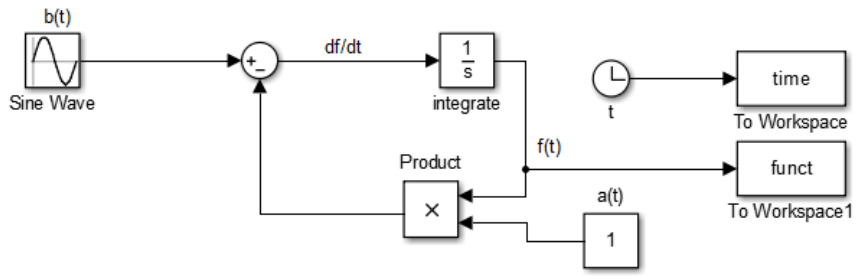

where, in particular, $a(t) = -1$ and $b(t) = \sin(t)$. It could be seen that there is a fulcrum in the whole representation: the algebraic summation block

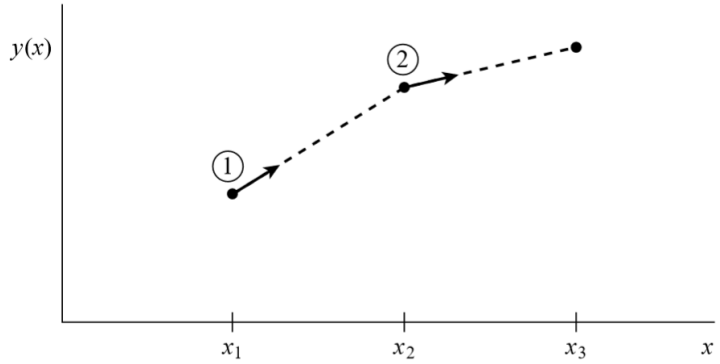

Figure 3.1: The Euler method is an easy, but less accurate, way to approximate the result function of a ODE. From [113].

which receives inputs from the b(t) block and the a·f(t) integration loop[1], and gives its output back to the numerical integration block.

Simulink® gives the possibility to choose between various integration methods: two methods which are commonly used in theoretical neuroscience are the Euler method and the derived Runge-Kutta method [110, 111, 112].

The Euler method The Euler method is probably the easiest method to estimate the behavior of an ODE

$$f(x_{n+1}) = f(x_n) + h \cdot g(x_n, f(x_n)), \quad \text{where } x_{n+1} = x_n + h \tag{3.2}$$

that is, the function f(x) is calculated in n+1 points on the x-axis with distance h, and at each point the function is approximated iteratively using adding h times the increase given by the tangent of the function in that point (Figure 3.1). The Euler method, even if commonly used in various simulations where the estimations could bear an error of the first order [93], is not very accurate[2] and could even show instabilities with *stiff* equations[3] [113].

[1]It is easily understandable that the loop takes the output from the summation block (namely, df/dt), integrates it through numerical integration ($\int$df/dtdt=f(t)) and the output undergoes a scalar product with a(t)–in case of a(t) being constant, or elementwise product otherwise–before getting subtracted to the updated df/dt.

[2]The error is of the O(h^2) order (i.e. the first order), that is if h=0.1 the error is of the order of 1% *for each step*!

[3]An ODE shows stiffness when its solution shows two very different behaviors (i.e. a reverse exponential rapidly going to zero and a 'standard' reverse exponential) for the same variable. For more details see [113].

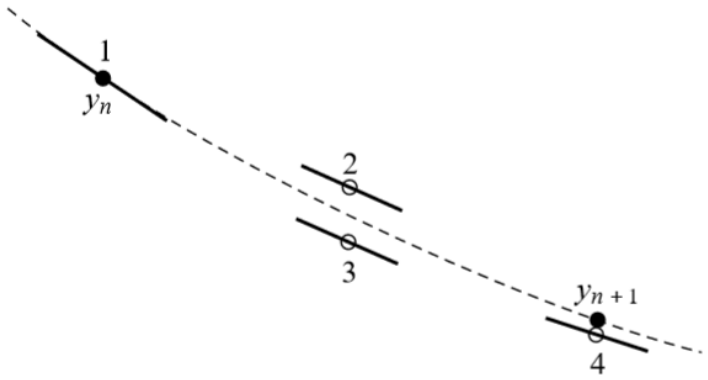

Figure 3.2: The fourth-order Runge-Kutta method is a standard simulation method for ODEs. From [113].

The Runge-Kutta method The idea underlying the Runge-Kutta method is to extend the accuracy of the Euler method (and thus to lessen the error) through the use of *virtual points* where to calculate the derivative, and then to use the intermediate steps to get the approximation [113]. The positions of the virtual midpoints should be so as to eliminate the lower order components of the error. For the *second-order Runge-Kutta* (RK) *method*, for example, the evaluation is made using the exact midpoint[4] of the Euler method:

$$k_1 = h \cdot g(x_n, f(x_n)) \tag{3.3}$$

$$f(x_{n+1}) + h \cdot g(x_n + \frac{h}{2}, f(x_n) + \frac{k_1}{2}), \quad where x_{n+1} = x_n + k. \tag{3.4}$$

The error of the approximation is $O(h^3)$, that is defined as a second-order[5] error. A higher-order[6] RK method can be extended with the proper modications to a fourth order formula [114]:

$$k_1 = h \cdot g(x, f(x_n)) \tag{3.5}$$

$$k_2 = h \cdot g(x_n + \frac{h}{2}, f(x_n) + \frac{k_1}{2} \tag{3.6}$$

[4]For this reason the second order Runge-Kutta method is also called *midpoint method* [113].

[5]In general an error of the n-order is given when the approximation on the variable x is cut at $O(x^{n+1})$.

[6]As William Press and colleagues pointed out in [113], a higher order of error does not necessarily mean a better accuracy from a mathematical point of view and a general point of view. There are specific features in the approximated functions which determine whether a fourth-order RK method gives better accuracy than the midpoint method, so the association higher order/higher accuracy is often valid, but surely not always.

$$k_3 = h \cdot g(x_n + \frac{h}{2}, f(x_n) + \frac{k_2}{2}) \tag{3.7}$$

$$k_4 = h \cdot g(x_n + h, f(x_n) + k_3) \tag{3.8}$$

$$f(x_{n+1}) = f(x_n) + \frac{k_1}{6} + \frac{k_2}{3} + \frac{k_3}{3} + \frac{k_4}{6}, \quad where x_{n+1} = x_n + k. \tag{3.9}$$

Obviously, a fourth order RK method have a $O(h^5)$ error per step and undergoes four steps of function derivation (Figure 3.2).

Simulation of ODEs using Simulink® Given the following simple ordinary differential equation

$$\frac{\mathrm{d}f(t)}{\mathrm{d}t} = -f(t) + \sin(t) \tag{3.10}$$

which was represented in the scheme at page 35, it would be easy to find that the analytic solution–with starting condition $f(t=0) = 0$–is[7]

$$f(t) = \frac{e^{-t}}{2} + \frac{\sin(t)}{2} - \frac{\cos(t)}{2}. \tag{3.11}$$

[7]The Equation 3.10 is a first-order, non homogeneous, linear differential equation. Here's a simple derivation through notation abuse:

$$\frac{\mathrm{d}f(t)}{\mathrm{d}t} = -f(t) + \sin(t)$$

Let's solve the associated homogeneous equation

$$\frac{\mathrm{d}f(t)}{\mathrm{d}t} = -f(t) \Rightarrow \frac{\mathrm{d}f(t)}{f(t)} = -\mathrm{d}t \Rightarrow \int \frac{\mathrm{d}f(t)}{f(t)} = -\int \mathrm{d}t$$

$$\ln(f(t)) + \chi = -t + \tau, \quad -\chi + \tau = \ln(c) \Rightarrow f(t) = c\,e^{-t}$$

Let's rearrange the non homogeneous equation:

$$\frac{\mathrm{d}f(t)}{\mathrm{d}t} + f(t) = \sin(t)$$

a guess of the solution can be made with the equation

$$f(t) = c\,e^{-t} + A\,\sin(t) + B\cos(t)$$

the substitution of the guess inside Equation 3.10 gives the values $A = \frac{1}{2}$ and $B = -\frac{1}{2}$. Now let's put the starting condition:

$$f(t=0) = c\,e^{0} + \frac{\sin(0)}{2} - \frac{\cos(0)}{2} = 0 \Rightarrow c = \frac{1}{2}$$

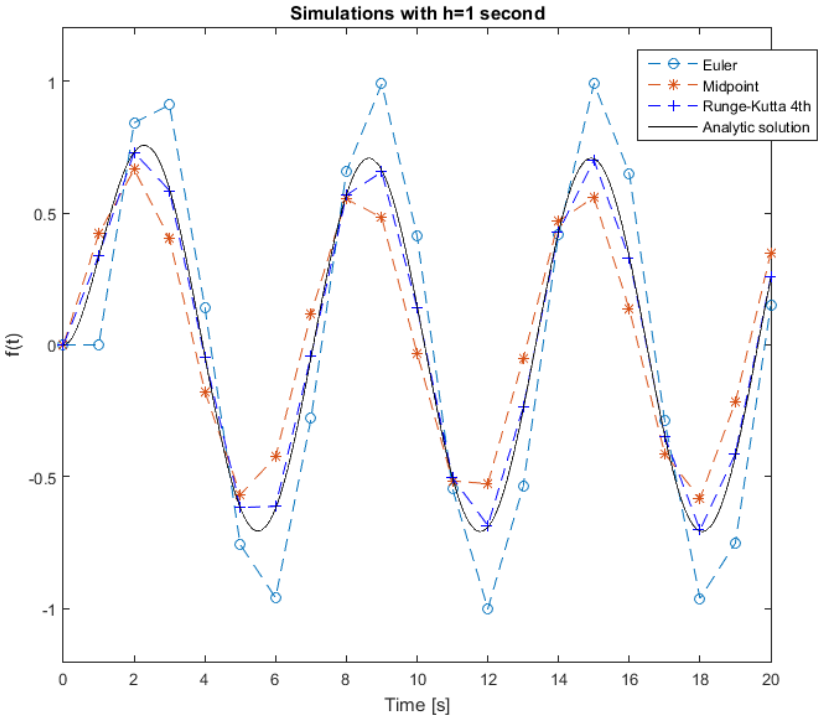

(a)

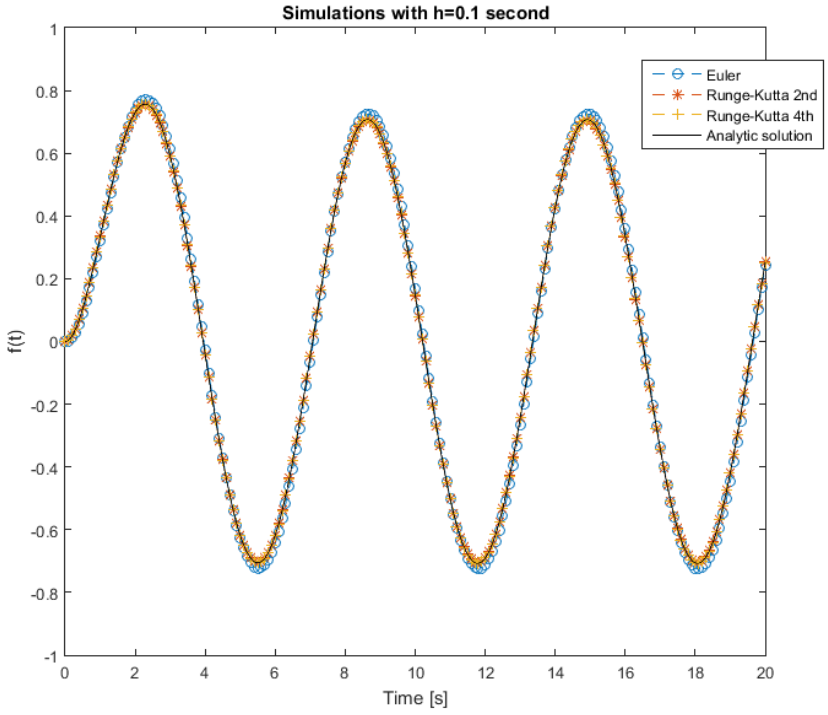

(b)

Figure 3.3: Simulations of the Equation 3.10 using different methods, compared to the analytic solution (Equation 3.11). (a) Using a step of h=1 evidences the limited accuracy of Euler method compared to higher-order Runge-Kutta methods, however when (b) the algorithm step becomes smaller h=0.1 each method gives as good an approximation as the others.

The Figure 3.3 summarize what it has been said so far about the different methods for ODEs simulation. First, it can be easily seen that the behavior of the simulations resemble closely the behavior of the exact solution. Moreover, it is visible that the correspondence between the order of the method and the accuracy of the simulation is strongly dependent[8] on the chosen h step (see also the note 6, page 37): a 'sufficiently small' h parameter would permit to use the Euler method and still to get a satisfyingly accurate result.

Now let's consider a more complex derivation of the Equation 3.1, such as the following

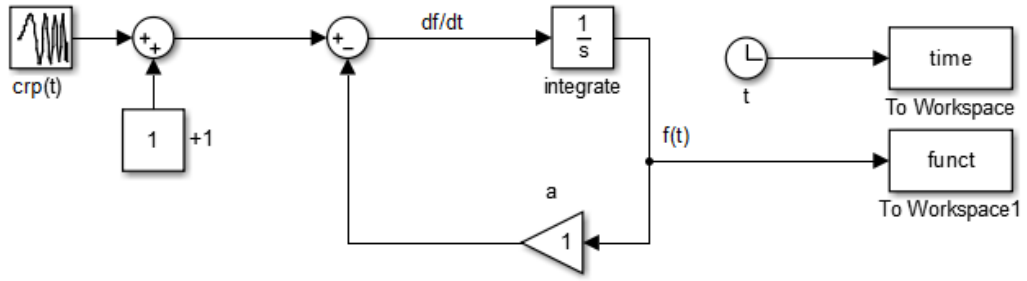

which would be described by the following equation:

$$\frac{\mathrm{d}f(t)}{\mathrm{d}t} = -f(t) + \mathrm{chirp}(t) + 1 \tag{3.12}$$

where chirp(t)+1 is a linear chirp function[9] with constant amplitude and which assumes always positive values. The Equation 3.12 would be a bit cumbersome to be solved analytically (if ever an exact solution exists), however its solution could be easily approximated using Simulink® numerical computing.

[8] Of course this is true only when non-pathological and non-stiff equations are considered.

[9] A chirp signal is a sinusolidal function whose instantaneous frequency changes from a start value ν_0 to an end value ν_1 in a time T [115]. In a linear chirp function the instantaneous frequency is described by the function

$$\nu(t) = \nu_0 + \frac{\nu_1 - \nu_0}{T}\, t$$

.

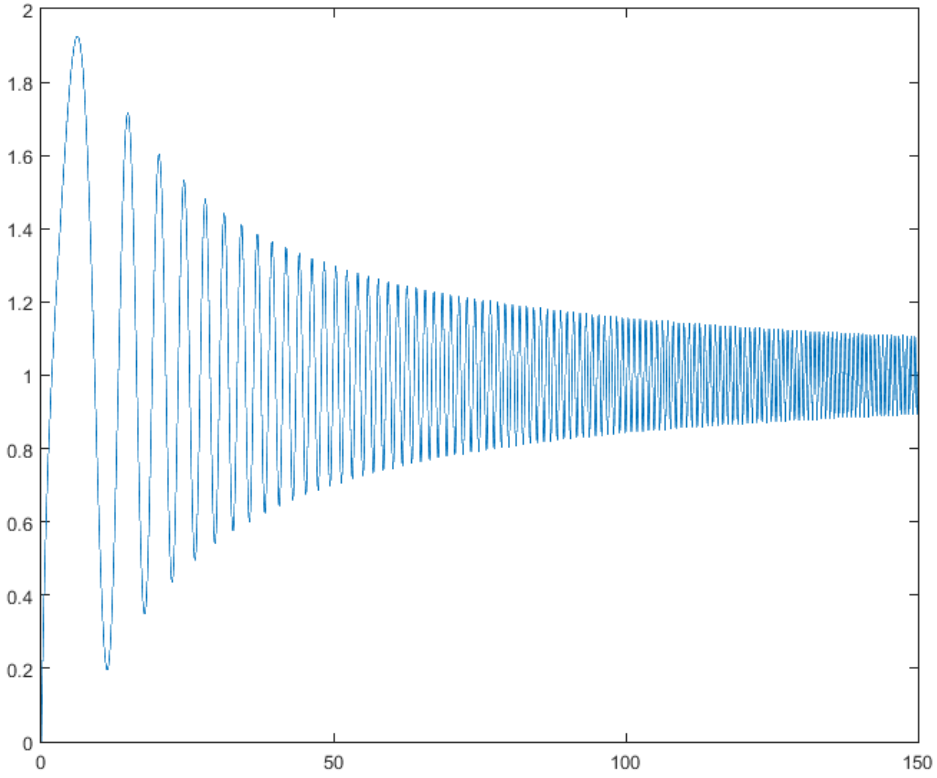

Figure 3.4: Approximated solution of the Equation 3.12: $\nu_0 = 0.2$Hz, $\nu_1 = 1$Hz $T = 100$s, fourth-order Runge-Kutta method with 0.01s time step.

The function plotted in Figure 3.4 shows two opposite moments of growth (led by the periodic function chirp$(t)+1$) and of relaxation (led by $-f(t)$). It is quite understandable that a system such the one generated by the general equation

$$\frac{\mathrm{d}f(t)}{\mathrm{d}t} = -|a(t)|f(t) + \mathrm{period}(t) \tag{3.13}$$

where period(t) is a periodic function, could present a situation where $|a(t)|f(t) =$ period(t). This property of the differential equation is called *averaging* [116], and usually occurs when period(t) shows a frequency which is bigger than a peculiar threshold frequency. From a signal processing point of view, when a system does averaging it roughly acts as a low-pass filter, so it increases the signal-to-noise ratio–*but only if the noise shows a high-frequency populated power spectrum*!

It would thus be of some interest to analyze the frequency-response properties of the PADP master equations (Equations 2.11 and 2.12), in order to check whether any low-pass filtering or averaging phenomenon occurs[10].

[10]A thoughtful reader could now ask why in this paragraph I just dealt with single

Implementation of the PADP equations The dynamic system that compose the PADP model (Equations 2.11 and 2.12) has been implemented in Simulink® according to the model shown in Figure 3.5. It can be seen that some components of the graphic model have been grouped together in an independent sub-model for many different reasons. The Orb2A aggregation (Figure 3.6A) is a 'not-necessary step' for the global functioning of the model[11] so the aggregation-related blocks can be clustered in a sub-group. The Heaviside-like functions (Figure 3.6B) can be logically considered a single block, so the grouping is just relevant to this purpose, while it is reasonable to separate the stimulation function (Figure 3.6C), whose form is chosen by the user[12], from the rest of the model.

ODE property analysis, and not with the analysis of dynamic systems–given that in the PADP model $[A] = [A](\sigma, [B^*], [A^*]$ and $[B^*] = [B^*]([A^*], \sigma)$. The main point about this problem, apart from the high level of complexity in studying the properties of non-linear dynamic systems, is that the peculiar switch-like nature of the Heaviside functions that mediate the relationship between $[A]$ and $[B^*]$ likely reduces their reciprocal influence. Actually, each equation which presents a Heaviside-like function could be substituted with a system of two equations and two conditions on the levels of the other protein–with the drawback of acquiring a point of discontinuity. So it is reasonable to claim that a great amount of properties of the Orb2 system could be studied at the level of the single master equation, though without neglecting the possible emergent properties that occur from the interaction of each equation which composes the model.

[11] Indeed, if one considered the aggregation propensity of Orb2A to be so high that every monomer enters immediately and permanently in an aggregate, the Orb2A aggregation step would be unnecessary, and the properties of the PADP model would barely change.

[12] For the PADP simulations I opted for a simple RC-like system, as in Equation 2.8, but it could be arbitrarily different.

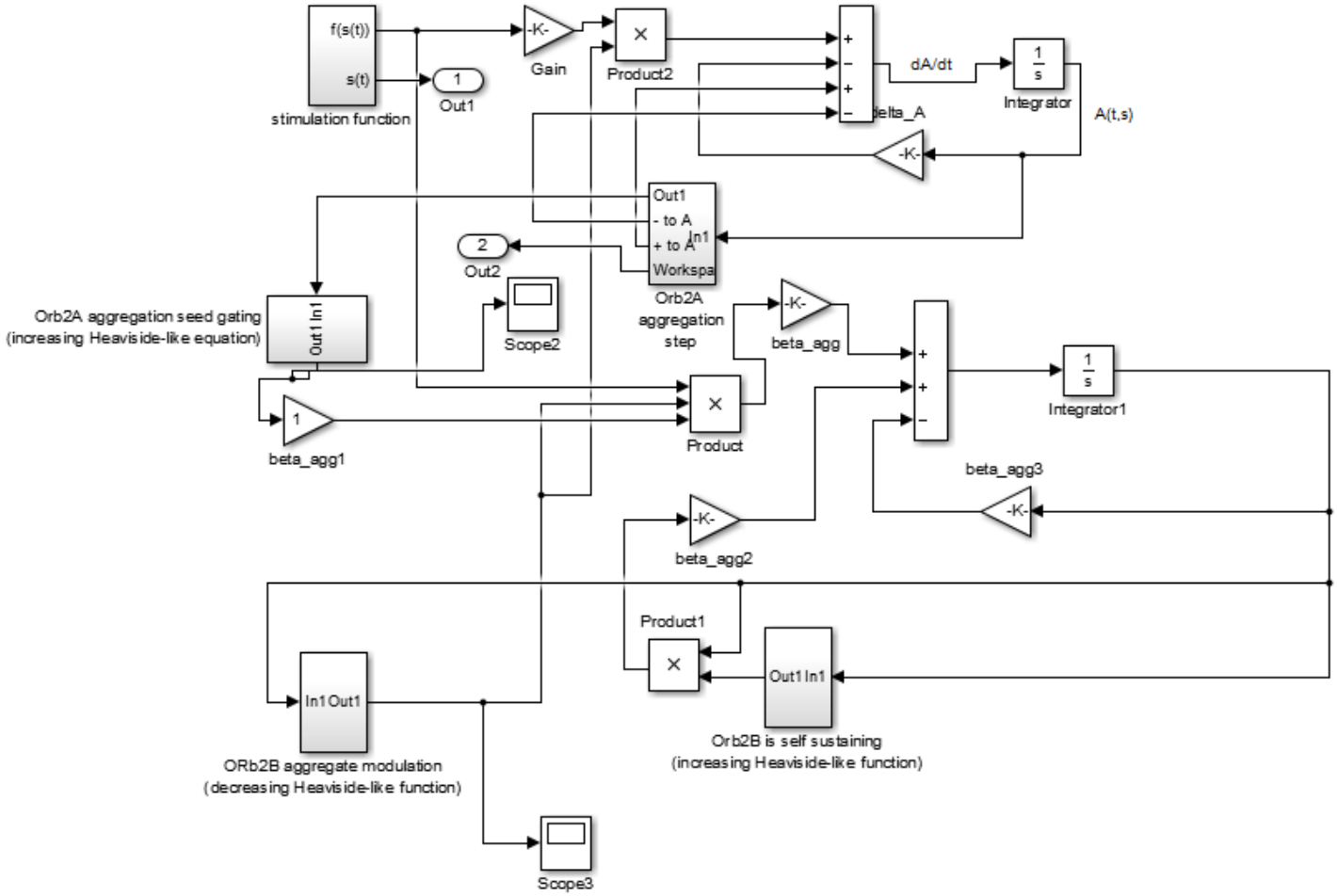

Figure 3.5: Simulink® graphical implementation of the PADP model equations (Eqn. 2.11 and 2.12). Some blocks were grouped together (stimulation process, aggregation, Heaviside-like threshold functions...).

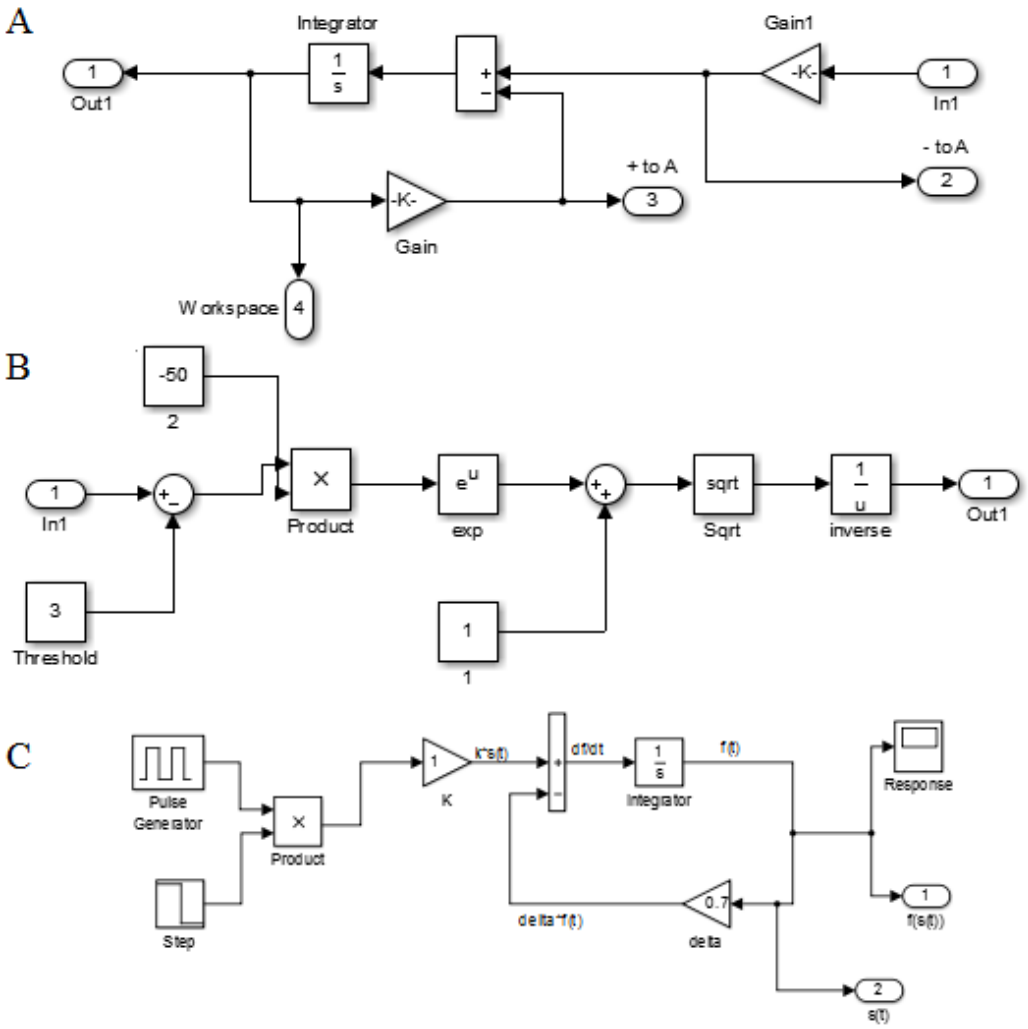

Figure 3.6: Scheme of A) the Orb2A aggregation subsystem, B) a Heaviside-like threshold function, and C) the function of synaptic activity $f(\sigma(t))$.

Chapter 4

Properties of the model

4.1 Numerical simulations

Numerical simulations of Equations 2.10, 2.12 and 4.1 were made using a Runge-Kutta fourth-order algorithm with an integration time step of 0.001 seconds and the parameters shown in **Table 4.1**. The Heaviside-like functions which were used for the simulations are continuous stepped functions:

$$\Theta^{0\to1}_{[A^*]}([A^*]) = \frac{1}{\sqrt{1+e^{-\alpha([A^*]-[A^*]_{\theta,min})}}} \tag{4.1}$$

$$\Theta^{0\to1}_{[B^*]}([B^*] = \frac{1}{\sqrt{1+e^{-\beta([B^*]-[B^*]_{\theta})}}} \tag{4.2}$$

$$\Theta^{1\to0}_{[B^*]}([B^*]) = \frac{1}{\sqrt{1+e^{\beta([B^*]-[B^*]_{\theta})}}} \tag{4.3}$$

where $\alpha, \beta \in \mathbb{N} : \alpha, \beta \gg 1$ in order to get a steep transition at the threshold and $[B^*]_\theta = [B^*]_{\theta,A} = [B^*]_{\theta,BA} = [B^*]_{\theta,BB}$ because I assume only one level of Orb2 aggregate-dependent regulation of Orb2A and Orb2B aggregation.

The stimulation pattern $\sigma(t)$ was a unit square wave function with 30% duty cycle and period T=5s. (The *duty cycle* of a square stimulus is the ratio of the period which is occupied by the stimulation.)

I then tested the model in order to assess: 1) the sensitivity to the length of the stimulation–that is, a short, spurious stimulation shouldn't trigger the long term facilitation–and 2) the self-limited growth even after a continuous stimulation. Figure 4.1 shows a simulation with 4000 s of stimulation time (a physiological-like contest) and the self-limiting behavior is visible. Figure 4.2 shows a simulation with 2000 s of stimulation time: since Orb2A levels haven't reached a sufficient level to form the aggregation seed, no aggregated Orb2B forms. Figure 4.3 shows a simulation with continuous stimulation:

Numerical values of parameters					
k_{on}	1	Hz	k_{off}	0.7	Hz
$\alpha_{\text{tr}} \cdot [\rho]_A$	0.005	$\frac{units}{s}$	α_{deg}	0.002	Hz
α_{agg}	0.008	Hz	α_{ex}	0.001	Hz
$[A^*]_\theta$	3	*units*			
β_{agg}	0.1	$\frac{units}{s}$	β_{ex}	0.0004	Hz
$[B^*]_\theta$	3	*units*			
α	50		β	50	

Table 4.1: Parameters of Orb2 model used in numerical simulations.

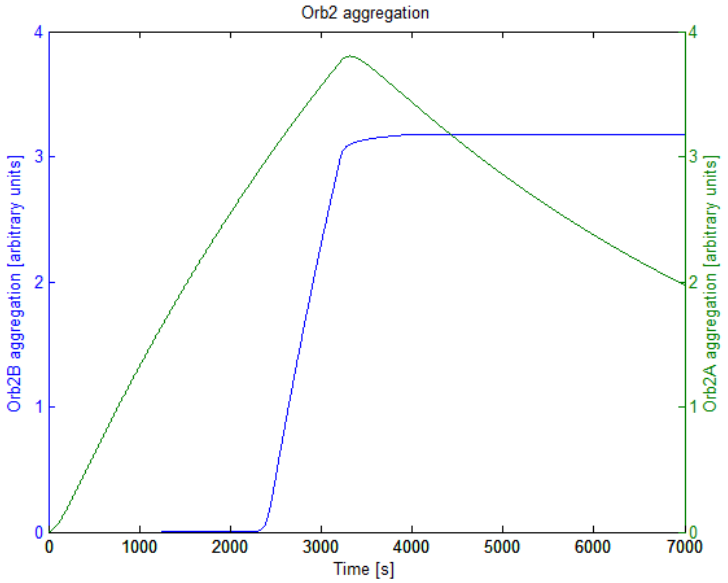

Figure 4.1: Simulation of the aggregation levels of Orb2B (blue) and Orb2A (green) with 4000s of binary square stimulation (T=5s, duty cycle 30%).

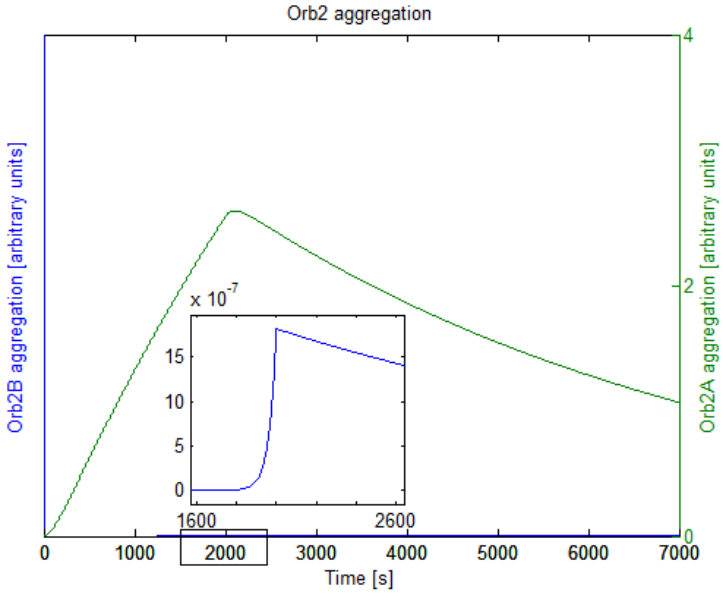

Figure 4.2: Simulation of the aggregation levels of Orb2B (blue) and Orb2A (green) with 2000s of binary square stimulation (T=5s, duty cycle 30%).

the aggregated Orb2B level reaches a steady-state dimension similar to the physiological one.

4.2 Dependency on the characteristics of the stimulus

I then asked how the model responds to different characteristics of the (binary) stimulus $\sigma(t)$. The numerical simulation were made using a 4th order Dormand-Prince solver with variable time step between 0.001 and 0.01 seconds; the stimulation functions were forced to zero after 4000 seconds (to assume a probably physiological-like environment). I first considered the dependency on the presentation "frequency" of a constant length square stimulus (in Figure 4.4, 1.5 seconds), which has been produced using a square function with varying period and duty cycle, in order to get a 1.5s stimulation followed by a uniformly distributed resting time. From Figure 4.4 it can be seen that there is a threshold of frequency (in this model being between 0.14 and 0.2 $\frac{\text{stimuli}}{\text{second}}$) which leads to the self-sustaining aggregation. It could be seen that the simulated stimulus has two different characteristics: the *period* of stimulus presentation (T) and the *duty cycle*, which is more generally a

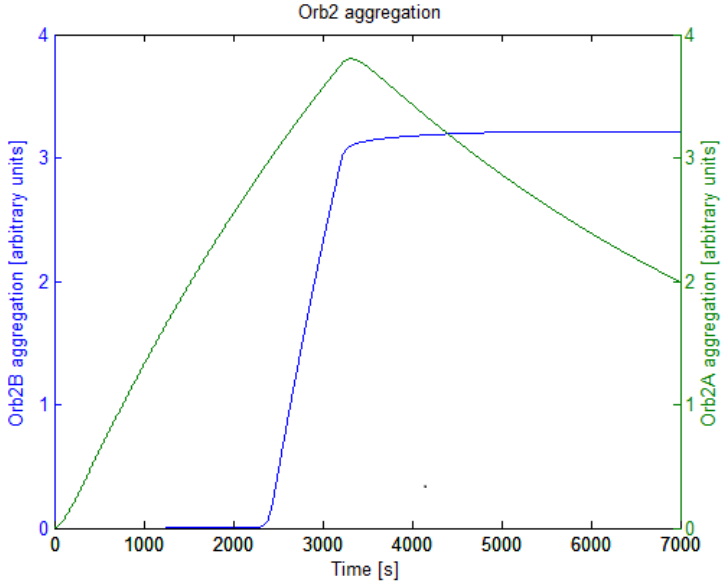

Figure 4.3: Simulation of the aggregation levels of Orb2B (blue) and Orb2A (green) with continuous binary square stimulation (T=5s, duty cycle 30%).

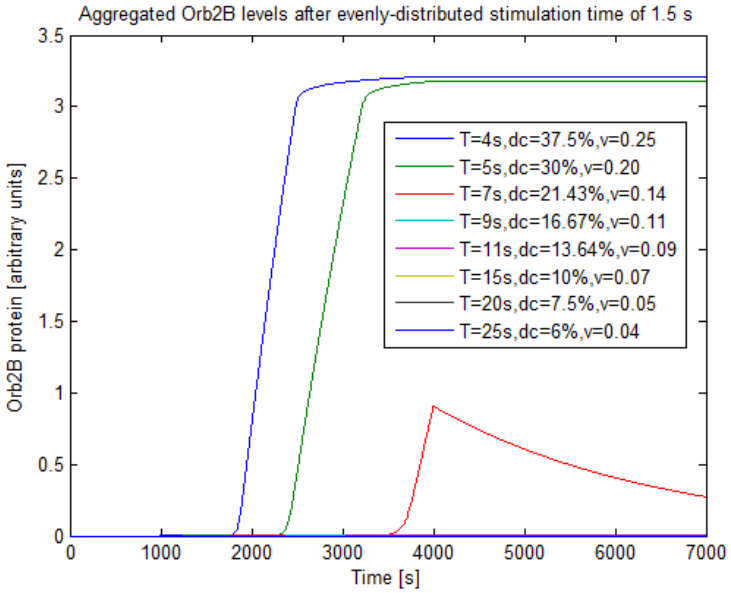

Figure 4.4: Simulation of the levels of aggregated Orb2B with fixed stimulation time of 1.5s and uniformly distributed variable resting time.

parameter of the time when the system is able to produce a maximal ON signal compared to the relaxing time (here it will be called *mean effective stimulation time*).

Figure 4.5 A shows a multiple simulation where the period was the same (5 seconds) and the duty cycle was changed and Figure 4.5 B shows a multiple simulation where the duty cycle was kept constant (27%) and the period was variable–a continuous stimulation and a random one (Bernoulli binary distribution, p=0.27) were used as a control. The simulations show that the system, as I modeled it, is sensitive to the mean effective stimulation time rather than the period of stimulation and that the responsiveness of the aggregation to a given duty cycle depends on the total time of stimulation. That is, if we consider again Figure 4.4, a rhythmic stimulation with frequency of $0.14\frac{\text{stimuli}}{\text{second}}$ which ceases after 4000s does not trigger the self-sustaining aggregation of Orb2B, but a prolonged stimulation could trigger the oligomerization (Figure 4.6).

The shown Orb2-inspired aggregation system reveals an intrinsic ability to sustain a long-term summation of the external stimuli and could act as an integrator of the past activity of the synapse. The summation could occur at the level of the stimulus function $f(\sigma)$, of the Orb2A-Orb2B oligomerization or at both levels. As it could be expected, Figure 4.7 shows that the function f(σ) sums the binary stimulus in continuous patterns. In order to assess the intrinsic summation ability of Orb2A-Orb2B I set $f(\sigma) = \sigma(t)$ and then tested the sensitivity of the system to both period and duty cycle (Figure 4.8 A and B) of the pure binary square stimulation. The simulations show that the modeled aggregation system can act as an intrinsic integrator of the synaptic stimuli.

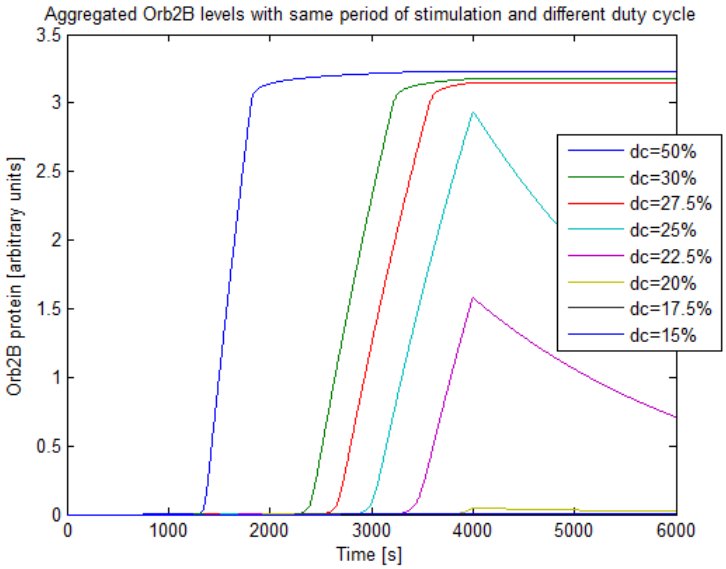

(a)

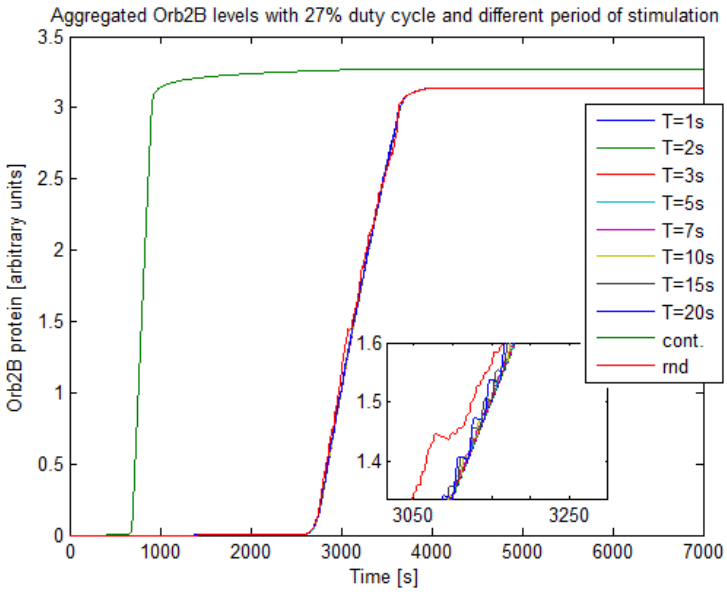

(b)

Figure 4.5: Multiple simulations of the levels of aggregated Orb2B with a) constant period T of 5s and variable duty cycle and b) constant duty cycle of 27% (close to the stabilization threshold) and variable period. There is a neat dependency of the aggregation of Orb2B from the mean effective stimulation time.

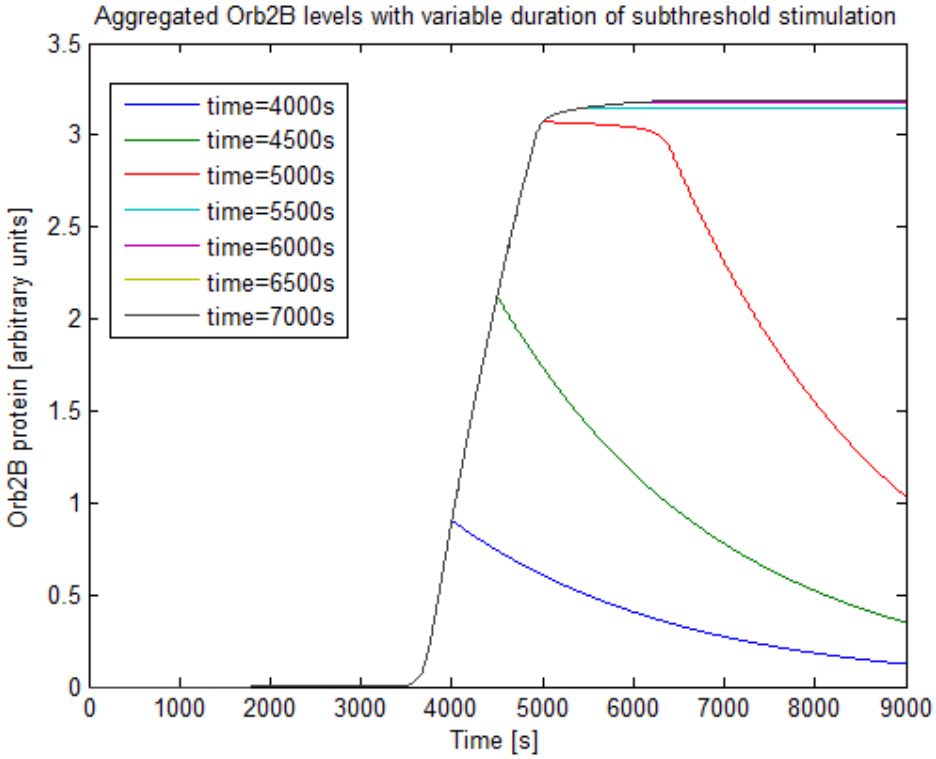

Figure 4.6: Multiple simulation where a 1.5s stimulus is presented with a frequency of $0.14\frac{\text{stimuli}}{\text{s}}$ for a variable total time. At 4000s (the stimulation time I used throughout the paper) the stimulus frequency is not sufficient to trigger the Orb2A-mediated Orb2B aggregation, however starting from 5500s it becomes sufficient.

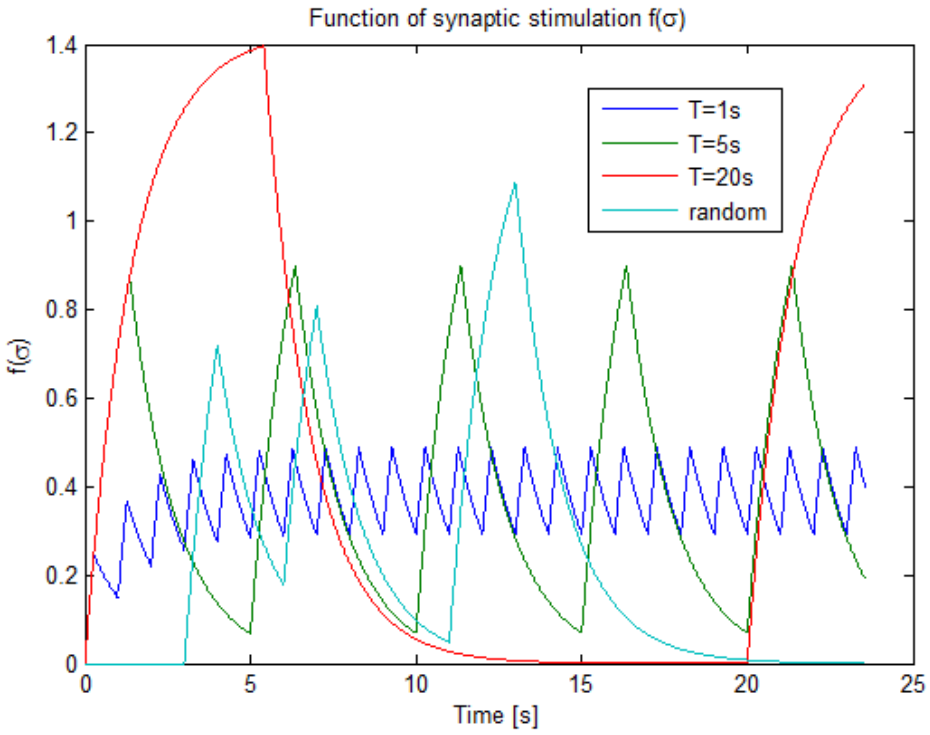

Figure 4.7: A brief interval of $f(\sigma, t)$ behavior according to Equation 8. The stimulation functions have a constant duty cycle (27%) and variable period (T). A multiform pattern of $\sigma(t)$ summation depending on T is visible.

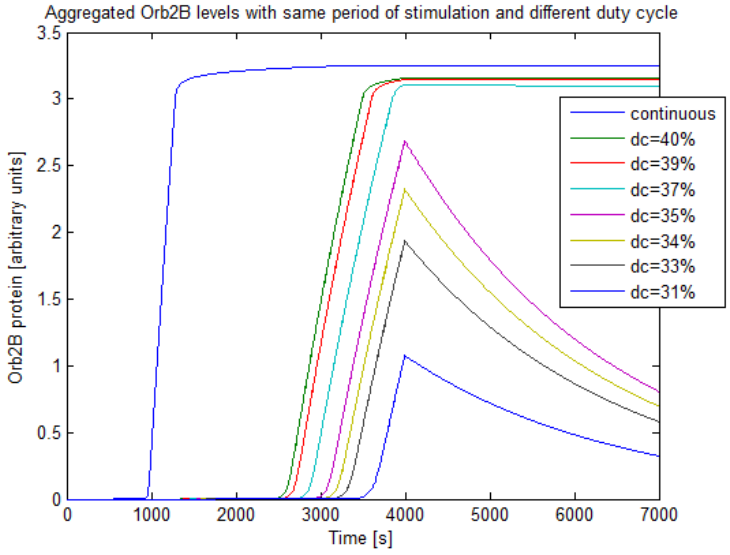

(a)

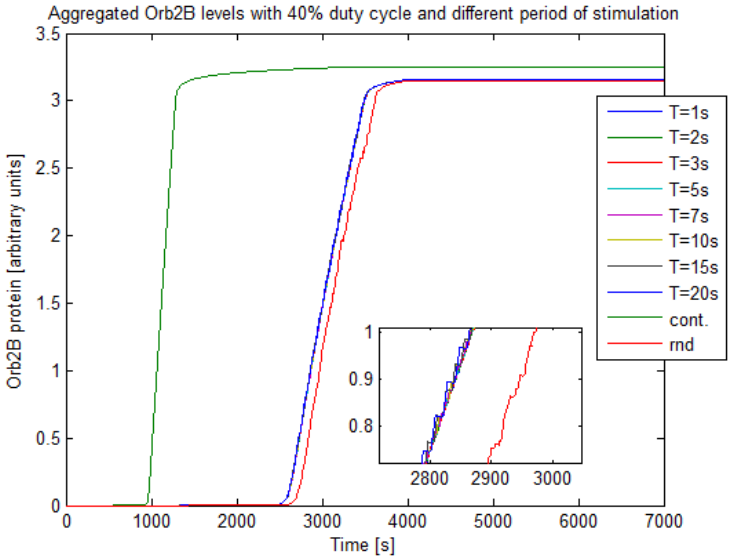

(b)

Figure 4.8: Multiple simulations of the levels of aggregated Orb2B with a binary square simulation of a) constant period T of 5s and variable duty cycle and b) constant duty cycle (40%) and variable period (T). In b) a continuous stimulation and a random stimulation (Bernoulli binary generator, p=0.4) were used as control. The simulations show an intrinsic ability of summation of the Orb2-inspired system.

Multiple values of parameters					
$\alpha_{\text{tr}} \cdot [\rho]_A$	α_{deg}	α_{agg}	α_{ex}	β_{agg}	β_{ex}
0.001	0.001	0.001	0.001	0.01	0.0001
0.01	0.01	0.01	0.01	0.1	0.001
0.1	0.1	0.1	0.1	1.0	0.01

Table 4.2: Parameters of Orb2 model used in multiple simulations.

Appendix: Stability of the simulations according to the model parameters

All the simulations that were presented in this chapter used the parameters written in Table 4.1 at page 46. These parameters were set manually according to three qualitative principles: 1) the simulation should not diverge (in particular, [A] and [A*] should not tend to $\pm\infty$), 2) the behavior of the model should resemble what is known for the behavior of the biological system, and 3) the relationship among the parameters should be biologically reasonable.

However, a possible criticism to this approach is that it is not clear whether the model shows a convergence behavior because this is a general property of the ODE system and not because it is a contingency due to the chosen parameters. In other words, there is the need to show the behavior of the model for different sets of parameters, and possibly to show which is the relationship between the different parameters and the dynamics of the system.

To test the model for multiple parameters, I set $f(\sigma, t)$ to be a bernoullian random number generator, the parameters of the Heaviside-like functions as in Table 4.1, and the total stimulation time to be 4000 sec. Three values for each parameter, spanning three orders of magnitude compared to the Table 4.1 parameters, were chosen[1] (see Table 4.2). The outcome of the system was measured at 7000 seconds, with the following approach:

- if $[B^*] < [B^*]_\theta$ and $0 \leq [A^*] \leq [A^*_\theta]$, the system was considered at *basal* state (i.e. non-facilitating);
- if $[B^*] \sim [B^*]_\theta$ and $0 \leq [A^*] \leq [A^*]_\theta$, the system was considered at *aggre-*

[1] Even using three values for each parameter, which could seem to be a narrow number of simulations, implies to simulate $3^6 = 729$ times the system shown in Figure 3.5. The computational burden of such an approach grows superlinearly $\propto x^6$, where x is the number of values for each parameter.

gated state (i.e. facilitating);

- if [A*]→ $+\infty$, or [A]→ $\pm\infty$ the system was considered *divergent* (i.e. underwent a pathological growth).

The following pie chart (Figure 4.9)) shows the distribution of the different outcomes in the simulations where each parameter assumed one of the values in Table 4.2. As it can be seen, a 24% of simulations resulted in a stable aggregate, thus meaning that the system has a certain attitude to converge to the $[B^*]_\theta$ value without showing a pathological growth of [A*].

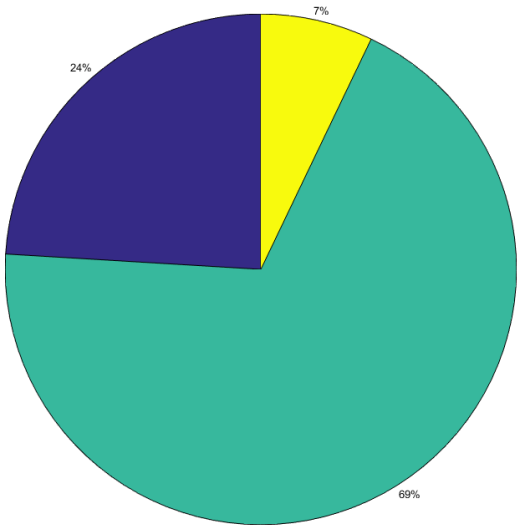

Figure 4.9: Pie chart which shows the percentage of the 729 simulations for the different outcomes. Cyan: 'basal', Blue: 'aggregated', Yellow:'divergent'.

The outcome of the multiple simulation is a function $\mathbb{R}^6 \to \mathbb{R}$, making impossible to plot at the same time how each parameter modifies the outcome of the model. In order to visualize the major effects of the different parameters I calculated the conditional probabilities that a parameter assumed a certain value, given that the model outcome is aggregated, basal or divergent (Table 4.3). From this approach, some properties of the system can be easily spotted, for example that the neat production rate of Orb2A is the first limiting factor which determines whether the model stays to a basal value or not[2], or the interplay between the Orb2A and the Orb2B aggrega-

[2]This is quite obvious: about half of the basal output simulations show the minimal production parameter (0.001, see Table 4.3). It is very interesting to see that the inverse conditional probability P(Agg| $\alpha_{\text{tr}} \cdot [\rho]_A$=0.001) is equal to 100%, that confirms the necessity to produce Orb2A in a sufficient amount in order to aggregate it...

Table 4.3: Conditioned probability (in %) for the different parameters, given a simulation outcome. Agg:aggregated, Bas: basal, Div:divergent.

$\alpha_{\text{tr}} \cdot [\rho]_A$			
	Bas	Agg	Div
0.001	48	0	0
0.01	32	39	29
0.1	20	61	71

α_{deg}			
	Bas	Agg	Div
0.001	34	47	76
0.01	33	36	22
0.1	33	17	2

α_{agg}			
	Bas	Agg	Div
0.001	46	18	2
0.01	46	35	27
0.1	7	46	71

α_{ex}			
	Bas	Agg	Div
0.001	38	47	76
0.01	31	36	22
0.1	31	17	2

β_{agg}			
	Bas	Agg	Div
0.01	36	21	59
0.1	33	37	29
1.0	31	43	12

β_{ex}			
	Bas	Agg	Div
0.0001	34	38	29
0.001	33	37	29
0.01	33	26	41

tion dynamics[3]. I then focused on which are the properties of the parameters that characterize a divergent behavior of the simulation, because there were only 51 permutations of the parameters of Table 4.2 which determined a divergent behavior, and they could be analyzed globally in order to find interesting patterns (Table 4.4). From visual inspection of Table 4.4, in fact, it can be seen that in divergent simulations there is a sort of imbalance between the production/degradation and aggregation/disaggregation reactions for Orb2A towards the production of ORb2A monomer and its aggregation (Figure 4.10 B). Interestingly, Figure 4.10 shows that, while the told imbalance towards Orb2A accumulation has a visible effect, there are probably more subtle effects arising from the combination of the different parameters in the model equations, that determine whether a group of balanced parame-

[3]Considering the conditional probabilities P(β_{agg} |Out) and P(β_{ex} |Out) (Table 4.3) is easy to see, for instance, that at low-levels of Orb2A aggregation ('basal' outcome) there is no influence of the β_{agg} and β_{ex} values. This independence holds also for the case of 'aggregated' outcome– with, of course, a slight bias towards higher values of β_{agg} and lower values of β_{ex}. It is interesting to notice a neat prevalence of the minimum value of β_{agg} (β_{agg}=0.01) in simulations with 'divergent' outcome, which mirrors the [B*] negative feedback on [A] production which I set in Equation 2.9. In the model, low values of Orb2B aggregation lead to a small inhibition of Orb2A production and thus a potentially explosive growth of [A] and [A*]–however this relationship is an arbitrary assumption, so it does not necessarily underlie a biological phenomenon.

Multiple values of parameters					
$\alpha_{\mathrm{tr}} \cdot [\rho]_A$	α_{deg}	α_{agg}	α_{ex}	β_{agg}	β_{ex}
0.01	0.001	0.01	0.001	0.01	0.0001
0.01	0.001	0.01	0.001	0.01	0.001
0.01	0.001	0.01	0.001	0.01	0.01
0.01	0.001	0.1	0.001	0.01	0.0001
0.01	0.01	0.1	0.001	0.01	0.0001
0.01	0.001	0.1	0.001	0.01	0.001
0.01	0.01	0.1	0.001	0.01	0.001
0.01	0.001	0.1	0.001	0.01	0.01
0.01	0.01	0.1	0.001	0.01	0.01
0.01	0.001	0.1	0.001	0.1	0.0001
0.01	0.001	0.1	0.001	0.1	0.001
0.01	0.001	0.1	0.001	0.1	0.01
0.01	0.001	0.1	0.01	0.01	0.0001
0.01	0.001	0.1	0.01	0.01	0.001
0.01	0.001	0.1	0.01	0.01	0.01
0.1	0.001	0.001	0.001	0.01	0.01
0.1	0.001	0.01	0.001	0.01	0.0001
0.1	0.001	0.01	0.001	0.01	0.001
0.1	0.001	0.01	0.001	0.01	0.01
0.1	0.01	0.01	0.001	0.01	0.01
0.1	0.001	0.01	0.001	0.1	0.0001
0.1	0.001	0.01	0.001	0.1	0.001
0.1	0.001	0.01	0.001	0.1	0.01
0.1	0.001	0.01	0.001	1.0	0.0001
0.1	0.001	0.01	0.001	1.0	0.001
0.1	0.001	0.01	0.001	1.0	0.01
0.1	0.001	0.01	0.01	0.01	0.01
0.1	0.001	0.1	0.001	0.01	0.0001
0.1	0.01	0.1	0.001	0.01	0.0001
0.1	0.001	0.1	0.001	0.01	0.001
0.1	0.01	0.1	0.001	0.01	0.001
0.1	0.001	0.1	0.001	0.01	0.01
0.1	0.01	0.1	0.001	0.01	0.01
0.1	0.1	0.1	0.001	0.01	0.01
0.1	0.001	0.1	0.001	0.1	0.0001
0.1	0.01	0.1	0.001	0.1	0.0001
0.1	0.001	0.1	0.001	0.1	0.001
0.1	0.01	0.1	0.001	0.1	0.001
0.1	0.001	0.1	0.001	0.1	0.01
0.1	0.01	0.1	0.001	0.1	0.01
0.1	0.001	0.1	0.001	1.0	0.0001
0.1	0.001	0.1	0.001	1.0	0.001
0.1	0.001	0.1	0.001	1.0	0.01
0.1	0.001	0.1	0.01	0.01	0.0001
0.1	0.001	0.1	0.01	0.01	0.001
0.1	0.001	0.1	0.01	0.01	0.01
0.1	0.01	0.1	0.01	0.01	0.01
0.1	0.001	0.1	0.01	0.1	0.0001
0.1	0.001	0.1	0.01	0.1	0.001
0.1	0.001	0.1	0.01	0.1	0.01
0.1	0.001	0.1	0.1	0.01	0.01

Table 4.4: Combination of parameters which determined a 'divergent' outcome.

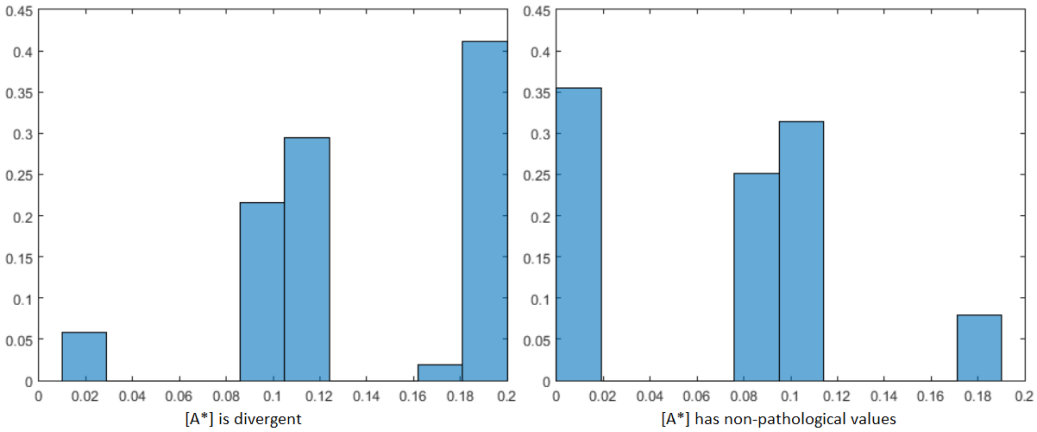

Figure 4.10: Histogram of the normalized frequency of given parameters combinations $(\alpha_{\text{tr}} \cdot [\rho]_A + \alpha_{\text{agg}})$-$(\alpha_{\text{deg}} + \alpha_{\text{ex}})$ in divergent and convergent simulations. There is an evident bias towards higher values (i.e. neat increase of [A] and [A*]) in the divergent simulations.

ters (with total summation close to zero) would converge to $[\text{B}^*]_\theta$ or diverge. The role of α_{ex} in determining the divergence of the simulations is important. In fact, when we are modeling very stable aggregates such as the amyloid oligomers there is a non-null possibility to set the 'oligomer-exit' parameter to zero, and this choice could thus potentially affect the global dynamics of the protein aggregation.

Chapter 5

Discussion and conclusions

I presented a model of continuous differential equations for the Orb2-mediated mechanisms of synaptic plasticity. This synaptic plasticity mechanism has been shown to be important for a paradigm of LTM in Drosophila, but the interest of aggregation-dependent synaptic plasticity goes beyond this specific example and could represent a more general mechanism. The simulations performed show that the model is consistent with the molecular behavior of Orb2 aggregates seen *in vitro* and *in vivo*. Orb2 protein aggregation is likely to be a detector of salient (i.e. biologically important) activity and a self-sustaining and self-limiting memory device whose outcome is very reliable and stable.

However, it is necessary to point out some limitations arising from such a model, because of the simplifying assumption I had to choose. Being a continuous model and considering the two states of the protein (free and aggregated) as two "compartments", the model does not take into account the probabilistic aspects of the local aggregation (for example the sensitivity to the fluctuations of protein concentration). Fluctuations in protein concentration might be particularly relevant, for the small volume and low protein numbers in the volume of a dendritic spine. Also, the model does not describe other kinetic aspects such as aggregate polarisation, the general mechanism of aggregation [117] and so on. Given the little knowledge of molecular interacting partners of the aggregate and the pathways of cellular regulation of Orb2 aggregates [95, 118] and the lack of a rigorous kinetic study of Orb2A-Orb2B homo- and hetero-induced aggregation, I found to be more conservative to model the overall known phenotype of Orb2 aggregate rather than to guess the molecular-level behaviour of the involved proteins. Other aspects of the model–now set as constant or null for simplicity's sake–that will have to be considered in future implementations of the model are the transition from a point synapse to a spatially extended one and a more complex dynamic

of Orb2A and Orb2B mRNAs and proteins, including diffusive components, RNA degradation, local depletion upon translation or aggregation, and so on. It would be surely significant to investigate a differential diffusivity between Orb2A or Orb2B free proteins and Orb2 aggregate–which *in vivo* probably characterizes the local (synaptic) specificity of PADP.

Another focal point in the model is the behavior of the aggregation according to the stimulation pattern. Using a binary periodic stimulation, I have shown that this system detects the likelihood of stimulation in a given time window, rather than the frequency of the stimulation *per se*. It has been shown that, during a spaced LTM-related training, there is the rise of a hours-long rhythmic dopaminergic stimulation which has a more uniform frequency spectrum and a higher amplitude than the basal state and could gate the transition between ARM and LTM [109]. If my assumptions are correct, the model would predict that the rhythmic stimulation should be permissive for the transition to LTM and the frequency of the stimulation wouldn't be instructive in this process, but it would be involved in reaching a sufficient level of stimulation during Orb2 aggregation time window. From an experimental point of view, this hypothesis could be assessed through, for example, the optogenetic control of specific populations of dopaminergic neurons in the mushroom body. Also, the model predicts that the Orb2 physiological aggregates at the synaptic level function as a high-pass filter which would discriminate the stronger, experience-evoked rhythmic stimulation from the spurious ones.

A further characteristic which emerged from the modeling is that the seeded aggregation process has an intrinsic ability to integrate the synaptic activity through time and locally. If this property was experimentally confirmed, the Orb2A-Orb2B system would extend the ability of synapses to integrate the information from the classic spatial cooperativity to a more complex spatio-temporal pattern.

The evidence of the Orb2 protein-only mechanisms involved in LTM could be used as an alternative to common synaptic facilitation rules such as the STDP [93] or the *Aplysia*-inspired activity-dependent presynaptic facilitation–ADPF [94]. STDP and ADPF are not self-regulating mechanisms, so they need extra-synaptic scaling mechanisms in order not to reach the synaptic saturation. The PADP does not incur in these limitations because it is based on a self-limiting aggregation process and lends itself to be heuristically applied in biological- and bioengineering-derived neural network simulations.

To my knowledge, this model is the first one which takes into account both protein aggregation as well as the local translation during synaptic facilitation processes. This approach could be further applied to other synaptic plastic-

ity phenomena which include local translation, such as the BDNF-induced plasticity [119] or mTORC-dependent plasticity [120]. There are other phenomena which are mediated by the formation of a stably active biological entity–just like the Orb2 functional amyloid–and are involved in memory induction and/or maintenance. A paradigmatic case, albeit controversial, is the kinase PKMζ, which is thought to be involved in memory long-term maintenance [46]. PKMζ is locally translated after a salient synaptic activity and is constitutively active (it does not rely on a secondary messenger to maintain its activity), in a way which is similar to the Orb2 aggregates here presented. Equations 2.5, 2.6 and 2.7 could be easily used as a starting point for a generalization of PADP in a plasticity rule which depends on synaptic protein network modification through local translation.

Bibliography

[1] E. R. Kandel, J. H. Schwartz, T. M. Jessell, *et al.*, *Principles of neural science*. McGraw-Hill New York, 2013.

[2] L. R. Squire, "Memory systems of the brain: A brief history and current perspective," *Neurobiology of Learning and Memory*, vol. 82, no. 3, pp. 171–177, 2004.

[3] J. L. Martinez Jr and B. E. Derrick, "Long-term potentiation and learning," *Annual review of psychology*, vol. 47, no. 1, pp. 173–203, 1996.

[4] H. Markram, W. Gerstner, and P. J. Sjstrm, "A history of spike-timing-dependent plasticity," *Frontiers in Synaptic Neuroscience*, vol. 3, no. 4, 2011.

[5] N. Le Novère, *Computational systems neurobiology*. Springer Science & Business Media, 2012.

[6] L. N. Cooper, "Stdp: spiking, timing, rates and beyond," *Frontiers in Synaptic Neuroscience*, vol. 2, no. 14, 2010.

[7] L. Squire, D. Berg, F. E. Bloom, S. du Lac, A. Ghosh, and N. C. Spitzer, *Fundamental neuroscience*. Academic Press, 2012.

[8] D. Hebb, *The Organization of Behaviour*. Wiley, 1949.

[9] K. Buchanan and J. Mellor, "The activity requirements for spike timing-dependent plasticity in the hippocampus," *Frontiers in Synaptic Neuroscience*, vol. 2, no. 11, 2010.

[10] D. Choquet and A. Triller, "The dynamic synapse.," *Neuron*, vol. 80, pp. 691–703, oct 2013.

[11] R. L. Huganir and R. a. Nicoll, "AMPARs and synaptic plasticity: the last 25 years.," *Neuron*, vol. 80, pp. 704–17, oct 2013.

[12] L. Fioriti, C. Myers, Y.-Y. Huang, X. Li, J. S. Stephan, P. Trifilieff, L. Colnaghi, S. Kosmidis, B. Drisaldi, E. Pavlopoulos, and E. R. Kandel, "The Persistence of Hippocampal-Based Memory Requires Protein Synthesis Mediated by the Prion-like Protein CPEB3," *Neuron*, pp. 1–16, 2015.

[13] M. Matsuzaki, N. Honkura, G. Ellis-Davies, and H. Kasai, "Structural basis of long-term potentiation in single dendritic spines," *Nature*, vol. 429, no. June, 2004.

[14] C. H. Bailey and E. R. Kandel, "Structural Changes Accompanying Memory Storage.," *Annual review of physiology*, vol. 55, pp. 397–426, 1993.

[15] L. Cooper, "A possible organization of animal memory and learning," in *Collective Properties of Physical Systems* (B. Lundqvist and S. Lundqvist, eds.), pp. 252–264, New York: Academic Press, 1973.

[16] R. W. Semon, *The mneme*. G. Allen & Unwin Limited, 1921.

[17] S. A. Josselyn, S. Köhler, and P. W. Frankland, "Finding the engram," *Nature Publishing Group*, vol. 16, no. 9, pp. 521–534, 2015.

[18] S. Ramirez, X. Liu, P.-A. Lin, J. Suh, M. Pignatelli, R. L. Redondo, T. J. Ryan, and S. Tonegawa, "Creating a false memory in the hippocampus.," *Science (New York, N.Y.)*, vol. 341, pp. 387–91, jul 2013.

[19] A. Hayashi-Takagi, S. Yagishita, M. Nakamura, F. Shirai, Y. I. Wu, A. L. Loshbaugh, B. Kuhlman, K. M. Hahn, and H. Kasai, "Labelling and optical erasure of synaptic memory traces in the motor cortex.," *Nature*, vol. 525, no. 7569, pp. 333–8, 2015.

[20] J. Sanes and J. Lichtman, "Can molecules explain long-term potentiation?," *Nature neuroscience*, pp. 597–604, 1999.

[21] T. Lømo, "The discovery of long-term potentiation," *Philosophical Transactions of the Royal Society B: Biological Sciences*, vol. 358, no. 1432, pp. 617–620, 2003.

[22] K. A. Goosens and S. Maren, "Long-term potentiation as a substrate for memory: Evidence from studies of amygdaloid plasticity and Pavlovian fear conditioning," *Hippocampus*, vol. 12, no. 5, pp. 592–599, 2002.

[23] R. a. Nicoll and K. W. Roche, "Long-term potentiation: peeling the onion.," *Neuropharmacology*, vol. 74, pp. 18–22, nov 2013.

[24] J. W. Rudy, *The neurobiology of learning and memory.* Sinauer, 2014.

[25] G. Neves, S. F. Cooke, and T. V. P. Bliss, "Synaptic plasticity, memory and the hippocampus: a neural network approach to causality.," *Nature reviews. Neuroscience*, vol. 9, no. 1, pp. 65–75, 2008.

[26] C. Brakebusch, C. I. Seidenbecher, F. Asztely, U. Rauch, H. Matthies, H. Meyer, M. Krug, T. M. Böckers, X. Zhou, M. R. Kreutz, *et al.*, "Brevican-deficient mice display impaired hippocampal ca1 long-term potentiation but show no obvious deficits in learning and memory," *Molecular and cellular biology*, vol. 22, no. 21, pp. 7417–7427, 2002.

[27] P. Park, A. Volianskis, T. M. Sanderson, Z. a. Bortolotto, D. E. Jane, M. Zhuo, B.-K. Kaang, and G. L. Collingridge, "NMDA receptor-dependent long-term potentiation comprises a family of temporally overlapping forms of synaptic plasticity that are induced by different patterns of stimulation.," *Philosophical transactions of the Royal Society of London. Series B, Biological sciences*, vol. 369, p. 20130131, jan 2014.

[28] D. Xia, H. Watanabe, B. Wu, S. H. Lee, Y. Li, E. Tsvetkov, V. Y. Bolshakov, J. Shen, and R. J. Kelleher, "Presenilin-1 Knockin Mice Reveal Loss-of-Function Mechanism for Familial Alzheimers Disease," *Neuron*, vol. 85, no. 5, pp. 967–981, 2015.

[29] H.-W. Chao, L.-Y. Tsai, Y.-L. Lu, P.-Y. Lin, W.-H. Huang, H.-J. Chou, W.-H. Lu, H.-C. Lin, P.-T. Lee, and Y.-S. Huang, "Deletion of CPEB3 enhances hippocampus-dependent memory via increasing expressions of PSD95 and NMDA receptors.," *The Journal of neuroscience : the official journal of the Society for Neuroscience*, vol. 33, no. 43, pp. 17008–22, 2013.

[30] A. Villers, E. Godaux, and L. Ris, "Long-lasting LTP requires neither repeated trains for its induction nor protein synthesis for its development.," *PloS one*, vol. 7, p. e40823, jan 2012.

[31] A.-K. Abbas, M. Dozmorov, R. Li, F.-S. Huang, F. Hellberg, J. Danielson, Y. Tian, J. Ekström, M. Sandberg, and H. Wigström, "Persistent LTP without triggered protein synthesis.," *Neuroscience research*, vol. 63, pp. 59–65, jan 2009.

[32] J. Lisman, "A mechanism for memory storage insensitive to molecular turnover," *Proceedings of the National Academy of Sciences of the United States of America*, vol. 82, no. May, pp. 3055–3057, 1985.

[33] K. Si, Y.-B. Choi, E. White-Grindley, A. Majumdar, and E. R. Kandel, "Aplysia CPEB can form prion-like multimers in sensory neurons that contribute to long-term facilitation.," *Cell*, vol. 140, pp. 421–35, Feb. 2010.

[34] T. J. Craddock, J. A. Tuszynski, and S. Hameroff, "Cytoskeletal signaling: is memory encoded in microtubule lattices by camkii phosphorylation," *PLoS Comput Biol*, vol. 8, no. 3, p. e1002421, 2012.

[35] S. Hameroff and R. Penrose, "Orchestrated reduction of quantum coherence in brain microtubules: A model for consciousness," *Mathematics and computers in simulation*, vol. 40, no. 3, pp. 453–480, 1996.

[36] J. H. Kotaleski and K. T. Blackwell, "Modelling the molecular mechanisms of synaptic plasticity using systems biology approaches," *Nature Reviews Neuroscience*, vol. 11, no. 4, pp. 239–251, 2010.

[37] U. S. Bhalla, "Trafficking motifs as the basis for two-compartment signaling systems to form multiple stable states.," *Biophysical journal*, vol. 101, pp. 21–32, jul 2011.

[38] A. Majumdar, W. C. Cesario, E. White-Grindley, H. Jiang, F. Ren, M. R. Khan, L. Li, E. M. L. Choi, K. Kannan, F. Guo, J. Unruh, B. Slaughter, and K. Si, "Critical role of amyloid-like oligomers of Drosophila Orb2 in the persistence of memory," *Cell*, vol. 148, no. 3, pp. 515–529, 2012.

[39] Y. Lu, Y. Ji, S. Ganesan, R. Schloesser, K. Martinowich, M. Sun, F. Mei, M. V. Chao, and B. Lu, "TrkB as a potential synaptic and behavioral tag.," *The Journal of neuroscience : the official journal of the Society for Neuroscience*, vol. 31, pp. 11762–71, aug 2011.

[40] L. H. Chao, P. Pellicena, S. Deindl, L. a. Barclay, H. Schulman, and J. Kuriyan, "Intersubunit capture of regulatory segments is a component of cooperative CaMKII activation.," *Nature structural & molecular biology*, vol. 17, pp. 264–72, mar 2010.

[41] J. Lisman, R. Yasuda, and S. Raghavachari, "Mechanisms of CaMKII action in long-term potentiation.," *Nature reviews. Neuroscience*, vol. 13, pp. 169–82, mar 2012.

[42] S.-J. R. Lee, Y. Escobedo-Lozoya, E. M. Szatmari, and R. Yasuda, "Activation of CaMKII in single dendritic spines during long-term potentiation.," *Nature*, vol. 458, pp. 299–304, mar 2009.

[43] K. C. Martin, A. Casadio, H. Zhu, Y. E, J. C. Rose, M. Chen, C. H. Bailey, and E. R. Kandel, "Synapse-Specific, Long-Term Facilitation of Aplysia Sensory to Motor Synapses: A Function for Local Protein Synthesis in Memory Storage," *Cell*, vol. 91, pp. 927–938, Dec. 1997.

[44] R. Malinow, H. Schulman, and R. W. Tsien, "Inhibition of postsynaptic PKC or CaMKII blocks induction but not expression of LTP.," *Science*, vol. 245, no. 4920, pp. 862–866, 1989.

[45] A. C. Newton, "Protein kinase c: structure, function, and regulation," *Journal of Biological Chemistry*, vol. 270, no. 48, pp. 28495–28498, 1995.

[46] J. L. Kwapis and F. J. Helmstetter, "Does pkm(zeta) maintain memory?," *Brain Research Bulletin*, vol. 105, no. 0, pp. 36 – 45, 2014. Mechanisms of memory enhancement and erasure.

[47] L. J. Volk, J. L. Bachman, R. Johnson, Y. Yu, and R. L. Huganir, "Pkmζ is not required for hippocampal synaptic plasticity, learning and memory," *Nature*, vol. 493, no. 7432, pp. 420–423, 2013.

[48] J. Greenwald and R. Riek, "Biology of amyloid: structure, function, and regulation.," *Structure (London, England : 1993)*, vol. 18, pp. 1244–60, oct 2010.

[49] T. P. J. Knowles, M. Vendruscolo, and C. M. Dobson, "The amyloid state and its association with protein misfolding diseases.," *Nature reviews. Molecular cell biology*, vol. 15, pp. 384–96, jun 2014.

[50] D. M. Fowler, A. V. Koulov, W. E. Balch, and J. W. Kelly, "Functional amyloid–from bacteria to humans.," *Trends in biochemical sciences*, vol. 32, pp. 217–24, may 2007.

[51] I. P. Pavlov and G. V. Anrep, *Conditioned Reflexes: An Investigation of the Physiological Activity of the Cerebral Cortex; Translated and Edited by GV Anrep.* Dover Publications, 1960.

[52] L. R. Squire and E. R. Kandel, *Memory: From mind to molecules.* Macmillan, 2000.

[53] D. Chain, A. Casadio, S. Schacher, A. Hegde, M. Valbrun, N. Yamamoto, A. Goldberg, D. Bartsch, E. Kandel, and J. Schwartz, "Mechanisms for generating the autonomous camp-dependent protein kinase required for long-term facilitation in aplysia," *Neuron*, vol. 22, no. 1, pp. 147–156, 1999.

[54] K. Si, M. Giustetto, A. Etkin, R. Hsu, A. M. Janisiewicz, M. C. Miniaci, J.-H. Kim, H. Zhu, and E. R. Kandel, "A Neuronal Isoform of CPEB Regulates Local Protein Synthesis and Stabilizes Synapse-Specific Long-Term Facilitation in Aplysia," *Cell*, vol. 115, pp. 893–904, Dec. 2003.

[55] A. Hegde, K. Inokuchi, W. Pei, A. Casadio, M. Ghirardi, D. Chain, K. Martin, E. Kandel, and J. Schwartz, "Ubiquitin c-terminal hydrolase is an immediate-early gene essential for long-term facilitation in aplysia," *Cell*, vol. 89, no. 1, pp. 115–126, 1997.

[56] A. Casadio, K. C. Martin, M. Giustetto, H. Zhu, M. Chen, D. Bartsch, C. H. Bailey, and E. R. Kandel, "A Transient, Neuron-Wide Form of CREB-Mediated Long-Term Facilitation Can Be Stabilized at Specific Synapses by Local Protein Synthesis," *Cell*, vol. 99, pp. 221–237, oct 1999.

[57] Frey and Morris, "Synaptic tagging and long-term potentiation," *Nature*, vol. 385, pp. 533–536, 1997.

[58] R. Redondo and R. Morris, "Making memories last: the synaptic tagging and capture hypothesis," *Nature Reviews Neuroscience*, vol. 12, no. 1, pp. 17–30, 2010.

[59] M. Doyle and M. a. Kiebler, "Mechanisms of dendritic mRNA transport and its role in synaptic tagging.," *The EMBO journal*, vol. 30, pp. 3540–3552, aug 2011.

[60] E. Tongiorgi, M. Righi, and A. Cattaneo, "Activity-Dependent Dendritic Targeting of BDNF and TrkB mRNAs in Hippocampal Neurons," vol. 17, no. 24, pp. 9492–9505, 1997.

[61] E. Tongiorgi, M. Armellin, P. G. Giulianini, G. Bregola, S. Zucchini, B. Paradiso, O. Steward, A. Cattaneo, and M. Simonato, "Brain-derived neurotrophic factor mRNA and protein are targeted to discrete dendritic laminas by events that trigger epileptogenesis.," *The Journal of neuroscience : the official journal of the Society for Neuroscience*, vol. 24, pp. 6842–6852, jul 2004.

[62] F. Zalfa, M. Giorgi, B. Primerano, and A. Moro, "The Fragile X Syndrome Protein FMRP Associates with BC1 RNA and Regulates the Translation of Specific mRNAs at Synapses," *Cell*, vol. 112, pp. 317–327, 2003.

[63] G. J. Bassell and S. T. Warren, "Fragile X syndrome: loss of local mRNA regulation alters synaptic development and function.," *Neuron*, vol. 60, pp. 201–14, oct 2008.

[64] L. Liu-Yesucevitz, G. J. Bassell, a. D. Gitler, a. C. Hart, E. Klann, J. D. Richter, S. T. Warren, and B. Wolozin, "Local RNA Translation at the Synapse and in Disease," *Journal of Neuroscience*, vol. 31, pp. 16086–16093, nov 2011.

[65] A. M. Krichevsky and K. S. Kosik, "Neuronal RNA granules: A link between RNA localization and stimulation-dependent translation," *Neuron*, vol. 32, no. 4, pp. 683–696, 2001.

[66] C. E. Holt and E. M. Schuman, "The central dogma decentralized: new perspectives on RNA function and local translation in neurons.," *Neuron*, vol. 80, pp. 648–57, oct 2013.

[67] L. E. Hake and J. D. Richter, "Cpeb is a specificity factor that mediates cytoplasmic polyadenylation during xenopus oocyte maturation," *Cell*, vol. 79, no. 4, pp. 617–627, 1994.

[68] T. Afroz, L. Skrisovska, E. Belloc, J. Guillén-Boixet, R. Méndez, and F. H. T. Allain, "A fly trap mechanism provides sequence-specific RNA recognition by CPEB proteins," *Genes and Development*, vol. 28, no. 13, pp. 1498–1514, 2014.

[69] S. Xu, N. Hafer, B. Agunwamba, and P. Schedl, "The CPEB Protein Orb2 Has Multiple Functions during Spermatogenesis in Drosophila melanogaster," *PLoS Genetics*, vol. 8, no. 11, 2012.

[70] C. Vogler, K. Spalek, A. Aerni, P. Demougin, A. Müller, K.-D. Huynh, A. Papassotiropoulos, and D. J.-F. de Quervain, "CPEB3 is associated with human episodic memory.," *Frontiers in behavioral neuroscience*, vol. 3, no. May, p. 4, 2009.

[71] S. Krüttner, L. Traunmüller, U. Dag, K. Jandrasits, B. Stepien, N. Iyer, L. G. Fradkin, J. N. Noordermeer, B. D. Mensh, and K. Keleman, "Synaptic Orb2A Bridges Memory Acquisition and Late Memory Consolidation in Drosophila," *Cell Reports*, pp. 1–13, 2015.

[72] K. Keleman, S. Krüttner, M. Alenius, and B. J. Dickson, "Function of the Drosophila CPEB protein Orb2 in long-term courtship memory.," *Nature neuroscience*, 2007.

[73] I. Letunic, T. Doerks, and P. Bork, "Smart: recent updates, new developments and status in 2015," *Nucleic acids research*, vol. 43, no. D1, pp. D257–D260, 2015.

[74] J. D. Richter, "Cpeb: a life in translation," *Trends in biochemical sciences*, vol. 32, no. 6, pp. 279–285, 2007.

[75] K. Si, S. Lindquist, and E. R. Kandel, "A Neuronal Isoform of the Aplysia CPEB Has Prion-Like Properties," *Cell*, vol. 115, no. 7, pp. 879–891, 2003.

[76] J. S. Stephan, L. Fioriti, N. Lamba, L. Colnaghi, K. Karl, I. L. Derkatch, and E. R. Kandel, "The CPEB3 Protein Is a Functional Prion that Interacts with the Actin Cytoskeleton," *Cell Reports*, pp. 1–14, 2015.

[77] Y.-S. Huang, M.-C. Kan, C.-L. Lin, and J. D. Richter, "CPEB3 and CPEB4 in neurons: analysis of RNA-binding specificity and translational control of AMPA receptor GluR2 mRNA.," *The EMBO journal*, vol. 25, no. 20, pp. 4865–4876, 2006.

[78] T. Mastushita-Sakai, E. White-Grindley, J. Samuelson, C. Seidel, and K. Si, "Drosophila Orb2 targets genes involved in neuronal growth, synapse formation, and protein turnover.," *Proceedings of the National Academy of Sciences of the United States of America*, vol. 107, pp. 11987–92, June 2010.

[79] P. Ciryam, G. Tartaglia, R. I. Morimoto, C. M. Dobson, and M. Vendruscolo, "Widespread Aggregation and Neurodegenerative Diseases Are Associated with Supersaturated Proteins," *Cell Reports*, vol. 5, no. 3, pp. 781–790, 2013.

[80] P. Ciryam, R. Kundra, R. I. Morimoto, C. M. Dobson, and M. Vendruscolo, "Supersaturation is a major driving force for protein aggregation in neurodegenerative diseases," *Trends in Pharmacological Sciences*, vol. 36, no. 2, pp. 72–77, 2015.

[81] D. M. Walther, P. Kasturi, M. Zheng, S. Pinkert, G. Vecchi, P. Ciryam, R. I. Morimoto, C. M. Dobson, M. Vendruscolo, M. Mann, and F. U. Hartl, "Widespread Proteome Remodeling and Aggregation in Aging C. elegans," *Cell*, vol. 161, no. 4, pp. 919–932, 2015.

[82] B. L. Raveendra, A. B. Siemer, S. V. Puthanveettil, W. a. Hendrickson, E. R. Kandel, and A. E. McDermott, "Characterization of prion-like

conformational changes of the neuronal isoform of Aplysia CPEB.," *Nature structural & molecular biology*, vol. 20, no. 4, pp. 495–501, 2013.

[83] A. Lupas, M. Van Dyke, J. Stock, *et al.*, "Predicting coiled coils from protein sequences," *Science*, vol. 252, no. 5009, pp. 1162–1164, 1991.

[84] F. Fiumara, L. Fioriti, E. R. Kandel, and W. a. Hendrickson, "Essential role of coiled coils for aggregation and activity of Q/N-rich prions and PolyQ proteins," *Cell*, vol. 143, no. 7, pp. 1121–1135, 2010.

[85] E. R. Kandel, I. Derkatch, and E. Pavlopoulos, "The role of functional prions in the persistence of memory storage," in *Proteopathic Seeds and Neurodegenerative Diseases*, pp. 131–152, Springer, 2013.

[86] S. Krüttner, B. Stepien, J. N. Noordermeer, M. a. Mommaas, K. Mechtler, B. J. Dickson, and K. Keleman, "Drosophila CPEB Orb2A mediates memory independent of Its RNA-binding domain.," *Neuron*, vol. 76, pp. 383–95, Oct. 2012.

[87] M. Heisenberg, "Mushroom body memoir: from maps to models.," *Nature reviews. Neuroscience*, 2003.

[88] G. Newquist, "Brain organization and the roots of anticipation in Drosophila olfactory conditioning," 2011.

[89] D. Owald, J. Felsenberg, C. B. Talbot, G. Das, E. Perisse, W. Huetteroth, and S. Waddell, "Activity of Defined Mushroom Body Output Neurons Underlies Learned Olfactory Behavior in Drosophila," *Neuron*, vol. 86, no. 2, pp. 417–427, 2015.

[90] J. Y. Yu, M. I. Kanai, E. Demir, G. S. X. E. Jefferis, and B. J. Dickson, "Cellular organization of the neural circuit that drives Drosophila courtship behavior," *Current Biology*, 2010.

[91] K. Keleman, E. Vrontou, S. Krüttner, J. Y. Yu, A. Kurtovic-Kozaric, and B. J. Dickson, "Dopamine neurons modulate pheromone responses in Drosophila courtship learning," *Nature*, vol. 489, no. 7414, pp. 145–149, 2012.

[92] Y. Aso, D. Hattori, Y. Yu, R. M. Johnston, N. A. Iyer, T.-T. B. Ngo, H. Dionne, L. F. Abbott, R. Axel, H. Tanimoto, and G. M. Rubin, "The neuronal architecture of the mushroom body provides a logic for associative learning.," *eLife*, vol. 3, p. e04577, 2014.

[93] P. Arena, L. Patané, V. Stornanti, P. S. Termini, B. Zäpf, and R. Strauss, "Modeling the insect mushroom bodies: Application to a delayed match-to-sample task," *Neural Networks*, 2013.

[94] D. Smith, J. Wessnitzer, and B. Webb, "A model of associative learning in the mushroom body," *Biological Cybernetics*, 2008.

[95] E. White-Grindley, L. Li, R. Mohammad Khan, F. Ren, A. Saraf, L. Florens, and K. Si, "Contribution of Orb2A Stability in Regulated Amyloid-Like Oligomerization of Drosophila Orb2," *PLoS Biology*, vol. 12, no. 2, 2014.

[96] N. Hosoda, Y. Funakoshi, M. Hirasawa, R. Yamagishi, Y. Asano, R. Miyagawa, K. Ogami, M. Tsujimoto, and S.-i. Hoshino, "Anti-proliferative protein Tob negatively regulates CPEB3 target by recruiting Caf1 deadenylase.," *The EMBO journal*, vol. 30, no. 7, pp. 1311–1323, 2011.

[97] J. S. Gill, *Nova Mediates Experience Dependent Processing of Orb2A mRNA*. PhD thesis, University of Kansas, 2013.

[98] C.-H. T. Webb, N. J. Riccitelli, D. J. Ruminski, and A. Lupták, "Widespread occurrence of self-cleaving ribozymes.," *Science (New York, N.Y.)*, vol. 326, no. 5955, p. 953, 2009.

[99] H. Olzscha, S. M. Schermann, A. C. Woerner, S. Pinkert, M. H. Hecht, G. G. Tartaglia, M. Vendruscolo, M. Hayer-Hartl, F. U. Hartl, and R. M. Vabulas, "Amyloid-like aggregates sequester numerous metastable proteins with essential cellular functions," *Cell*, vol. 144, no. 1, pp. 67–78, 2011.

[100] M. R. Khan, L. Li, C. Pérez-Sánchez, A. Saraf, L. Florens, B. D. Slaughter, J. R. Unruh, and K. Si, "Amyloidogenic Oligomerization Transforms Drosophila Orb2 from a Translation Repressor to an Activator," *Cell*, vol. 163, no. 6, pp. 1468–1483, 2015.

[101] N. Hafer, S. Xu, K. M. Bhat, and P. Sched, "The drosophila CPEB protein orb2 has a novel expression pattern and is important for asymmetric cell division and nervous system function," *Genetics*, vol. 189, no. 3, pp. 907–921, 2011.

[102] G. U. Busto, I. Cervantes-Sandoval, and R. L. Davis, "Olfactory learning in Drosophila.," *Physiology (Bethesda, Md.)*, vol. 25, no. 6, pp. 338–346, 2010.

[103] S. Zhang and G. Roman, "Presynaptic inhibition of gamma lobe neurons is required for olfactory learning in Drosophila," *Current Biology*, vol. 23, no. 24, pp. 2519–2527, 2013.

[104] K. Gehring, K. Heufelder, and D. Eisenhardt, "Localization of phosphorylated creb in the honeybee brain," *Frontiers in Behavioral Neuroscience. Conference Abstract: Tenth International Congress of Neuroethology*, no. 149, 2012.

[105] B. Drisaldi, L. Colnaghi, L. Fioriti, N. Rao, C. Myers, A. M. Snyder, D. J. Metzger, J. Tarasoff, E. Konstantinov, P. E. Fraser, J. L. Manley, and E. R. Kandel, "SUMOylation Is an Inhibitory Constraint that Regulates the Prion-like Aggregation and Activity of CPEB3," *Cell Reports*, vol. 11, no. 11, pp. 1694–1702, 2015.

[106] D. N. Woolfson, "The design of coiled-coil structures and assemblies," *Advances in protein chemistry*, vol. 70, pp. 79–112, 2005.

[107] B. Almeida, I. A. Abreu, C. A. Matos, J. Fraga, S. Fernandes, M. G. Macedo, R. Gutiérrez-Gallego, P. J. B. Pereira, A. L. Carvalho, and S. Macedo-Ribeiro, "SUMOylation of the brain-predominant Ataxin-3 isoform modulates its interaction with p97.," *Biochimica et biophysica acta*, vol. 1852, no. 9, pp. 1950–1959, 2015.

[108] G. Isabel, A. Pascual, and T. Preat, "Exclusive consolidated memory phases in *Drosophila*," *Science*, vol. 304, no. 5673, pp. 1024–1027, 2004.

[109] P.-Y. Plaçais, S. Trannoy, G. Isabel, Y. Aso, I. Siwanowicz, G. Belliart-Guérin, P. Vernier, S. Birman, H. Tanimoto, and T. Preat, "Slow oscillations in two pairs of dopaminergic neurons gate long-term memory formation in Drosophila," *Nature Neuroscience*, vol. 15, no. 4, pp. 592–599, 2012.

[110] D. Hansel, G. Mato, C. Meunier, and L. Neltner, "On numerical simulations of integrate-and-fire neural networks," *Neural Computation*, vol. 10, no. 2, pp. 467–483, 1998.

[111] P. Dayan and L. F. Abbott, *Theoretical neuroscience*. MIT Press, 2001.

[112] E. M. Izhikevich, *Dynamical systems in neuroscience*. MIT press, 2007.

[113] W. H. Press, S. A. Teukolsky, W. T. Vetterling, and B. P. Flannery, *Numerical recipes in C*. Cambridge university press, 1992.

[114] M. Abramowitz and I. A. Stegun, *Handbook of mathematical functions: with formulas, graphs, and mathematical tables*. No. 55, Courier Corporation, 1964.

[115] T. Dau, O. Wegner, V. Mellert, and B. Kollmeier, "Auditory brainstem responses with optimized chirp signals compensating basilar-membrane dispersion.," *The Journal of the Acoustical Society of America*, vol. 107, no. March, pp. 1530–1540, 2000.

[116] Z. Artstein, "Averaging of time-varying differential equations revisited," *Journal of Differential Equations*, vol. 243, no. 2, pp. 146–167, 2007.

[117] S. I. Cohen, M. Vendruscolo, M. E. Welland, C. M. Dobson, E. M. Terentjev, and T. P. Knowles, "Nucleated polymerization with secondary pathways. i. time evolution of the principal moments," *The Journal of chemical physics*, vol. 135, no. 6, p. 065105, 2011.

[118] S. Kimura, Y. Sakakibara, K. Sato, M. Ote, H. Ito, M. Koganezawa, and D. Yamamoto, "The Drosophila lingerer protein cooperates with Orb2 in long-term memory formation.," *Journal of neurogenetics*, vol. 7063, no. 1, pp. 1–10, 2014.

[119] E. M. Schuman, J. L. Dynes, and O. Steward, "Synaptic regulation of translation of dendritic mRNAs.," *The Journal of neuroscience : the official journal of the Society for Neuroscience*, vol. 26, pp. 7143–7146, July 2006.

[120] J. O. Lipton and M. Sahin, "The Neurology of mTOR," *Neuron*, vol. 84, pp. 275–291, Oct. 2014.